HIGHLY PATHOGENIC AVIAN INFLUENZA H5N2 IN NATURALLY INFECTED TURKEY BREEDER HENS: VIRUS DISTRIBUTION, HISTOPATHOLOGY, AND HOST IMMUNE GENE EXPRESSION

A Dissertation

by

MICHELLE A. BEHL

Submitted to the Office of Graduate and Professional Studies of
Texas A&M University
in partial fulfillment of the requirements for the degree of

DOCTOR OF PHILOSOPHY

Chair of Committee,	David Caldwell
Co-Chair of Committee,	Michael Kogut
Committee Members,	Kenneth Gennovese
	Luc Berghman
	Morgan Farnell
Head of Department,	David Caldwell

August 2016

Major Subject: Poultry Science

ABSTRACT

The outbreak of the highly pathogenic avian influenza virus (HPAI) in 2014-2015 was by far the largest animal disease outbreak in United States history. The turkey industry was the most affected as nearly 70% of the confirmed cases were in turkeys. This project examined viral distribution, semi-quantitative viral load, histological viral lesions, and gene expression of several immune components in 8 tissues of naturally infected turkey breeder hens during the outbreak. Tissues from clinically and sub-clinically affected turkeys, as well as negative controls were obtained: brain, heart, GI, liver, lung, reproductive tract, spleen, and trachea. Changes in the gene expression of IL-1β, IL-6, IL-10, CCL-5, CXCLi-2, Mx, OASL, IFN-γ, IFIH1, FasL and TRAIL were described.

The matrix gene was detected in all 8 of the tissues collected from the clinical and sub-clinical groups. The clinically affected turkeys had significantly higher levels of matrix gene detected in the brain, GI, spleen, and trachea. Histological viral lesions were in general very mild and insignificant. The majority of the histological changes were confined to the trachea and liver and primarily consisted of the infiltration of small numbers of heterophils, lymphocytes, and macrophages. This particular virus was able to evade the host's immune response using several tactics. It was able to avoid initial detection by suppressing IFIH1 expression, the pro-inflammatory cytokines IL-1β and IL-6, and the antiviral component IFN-γ in the trachea. Undetected, the virus quickly

disseminated throughout the body and replicated rapidly. The widespread downregulation of IFN-γ and upregulation of CCL-5 and OASL likely contributed to the pathogenesis.

Virus was detected in all of the tissues collected on the positive premise, regardless of clinical status thus illustrating its extreme infectivity. Generally, histological lesions were minimal and cytokine responses were not excessive. Death does not appear to be the result of organ damage/necrosis or even cytokine storm, but purely from immune evasion and excessive viral load in the tissues. Consequently the high viral loads in the tissues resulted in organ failure.

DEDICATION

I dedicate this dissertation to my wonderful husband, John, and beautiful daughters, Adriana and Abigail. I want to thank them for their patience, understanding, and never-ending support and encouragement throughout this journey. My girls provided the strength and love that I needed to push through the difficult times, whether it was an encouraging picture on the wall, a cheer for my next exam, or a hug, they were always there to keep me going. I will never be able to express my love and gratitude to my husband for allowing me to chase my dreams. With love, anything is possible. He never once gave up on me or stopped believing in me. He was and will forever be my rock that helps me keep it all together.

The driving force behind my PhD has been to give something meaningful, significant, and applicable back to the turkey industry. The turkey industry is a relatively small industry and often times not at the forefront of poultry research for most scientists, due to time and costs. The outbreak of HPAI H5N2 was devastating on both a professional and personal level. I saw the outbreak as an opportunity and was determined to bring something good or useful out of the devastation with hopes that we may not have to experience it ever again.

ACKNOWLEDGEMENTS

I would like to thank my committee chair, Dr. Caldwell, my committee co-chair Dr. Kogut, and my committee members, Dr. Genovese, Dr. Berghman, and Dr. Farnell, for their guidance and support throughout the course of this research.

I want to thank Willmar Poultry dba Ag Forte for all of their support. Without them, this dream would not have been possible. I am forever indebted to them. I also want to thank all of my colleagues within the Ag Forte system as well as in the rest of the industry for their support and encouragement. During the most difficult times, I had an entire sideline of people cheering me on. It was those individuals that helped me push through. In particular, I want to thank Dr. Dave Fernandez for all of his guidance throughout the years. My appreciation goes to Baker Turkey Farm and Brian Orsten Turkeys for their support and access to birds for the study.

I cannot express my gratitude to Dr. Zheng Xing at the University of Minnesota for all of his guidance and assistance with the cytokine research. Thanks also goes to Dr. Carol Cardona, Cristian Florez Figuerosa, and Jennette Munoz Aguayo for their assistance at MCROC. I also want to acknowledge Dr. Daniel Shaw at the University of Missouri for this assistance with the histopathology.

Finally, I want to thank my family, particularly my parents, sister, nieces, and in-laws for their support and encouragement. I will never be able to thank them enough. Words will never be able to express my gratitude to my husband and children for all of the sacrifices they have made.

NOMENCLATURE

AI	Avian Influenza
APHIS	Animal and Plant Health Inspection Service
CC/CXC	Chemokine
Ct	Cycle Threshold
FADD	Fas-Associated Death Domain
FAO	Food and Agricultural Organization of the United Nations
FasL	CD95L
GAPDH	Glyceraldehyde 3-Phosphate Dehydrogenase
HA	Hemagglutinin
HI	Haemagglutination-Inhibition
HPAI	Highly Pathogenic Avian Influenza
IFIH1	Interferon–Induced Helicase Domain- containing protein 1
IFITM	Interferon-Induced Transmembrane Protein
IFN	Interferon
IL	Interleukin
IVIP	Intravenous Pathogenicity Index
LPAI	Low Pathogenic Avian Influenza
M gene	Matrix Gene
MDA5	Melanoma Differentiation-Associated Gene 5
Mx	Myxovirus-Resistance
NA	Neuraminidase

NI	Neuraminidase-Inhibition
NS	Nonstructural Protein
OAS	2’5’-Oligoadenylate Synthetase
OIE	Office International des Epizooties/World Organisation for Animal Health
PAMPs	Pathogen-Associated Molecular Patterns
PCR	Polymerase Chain Reaction
PRR	Pattern Recognition Receptors
RIG-I	Retinoic Acid-Inducible Gene I
rRT-PCR	Real Time Reverse Transcribed Polymerase Chain Reaction
Th	T-helper
TLR	Toll-like Receptors
TNF	Tumor Necrosis Factor
TRAIL	TNF- Related Apoptosis-Inducing Ligand
USDA	United States Department of Agriculture

TABLE OF CONTENTS

Page

LIST OF FIGURES

Page

LIST OF TABLES

Page

CHAPTER I

INTRODUCTION/LITERATURE REVIEW

History of Highly Pathogenic Avian Influenza

Highly Pathogenic Avian Influenza, formerly termed 'fowl plague', was first described in chickens in Italy by Perroncito in 1878 (Kaleta and Rulke, 2008). Although the disease quickly spread through Europe thereafter, it wasn't until 1901 that the disease was determined to be caused by a virus. The virus was not identified or classified until 1955. There have been 19 HPAI outbreaks worldwide since its classification, with the majority occurring in Europe and Asia (Swayne and Suarez, 2000; Swayne, 2008). The phrase 'highly pathogenic avian influenza' was coined in 1981 at the first International Symposium on Avian Influenza (Swayne and Suarez, 2000). Since then, there has been an intense international effort led by the Office International des Epizooties (OIE) and the Food and Agricultural Organization of the United Nations (FAO) to control and quickly eradicate the disease when necessary. Full eradication is not possible, since wild birds harbor and spread the virus. The United States' stringent 'stamping-out' policy for controlling HPAI contains the disease but results in significant direct and indirect loses to the industry and consumers via flock depopulation, disposal, quarantine, and cleaning and disinfection of infected flocks and premises (USDA-APHIS, 2015).

Prior to the outbreak of HPAI in the spring of 2015, there were three large HPAI outbreaks and a handful of smaller HPAI cases in the United States. The first outbreak of HPAI occurred in the fall and winter 1924-1925. The disease spread rapidly from live bird markets to other regions with the movement of infected birds and contaminated equipment (Lupiani and Reddy, 2009). Restrictions on the movement of live poultry and stringent quarantine, depopulation, and cleaning and disinfecting procedures controlled the outbreak and eradicated the disease from the United States (Lupiani and Reddy, 2009). The second HPAI outbreak in the United States was a result of an LPAI strain of H5N2 mutating into an HPAI strain. The outbreak was isolated to the northeastern states in 1983-1984 and involved more than 17 million birds (Lupiani and Reddy, 2009). The third HPAI outbreak occurred in a chicken flock in the southern United States in 2004 but was quickly eradicated (USDA, 2015).

Due to the deadly potential of AI, certain strains are notifiable to the World Organisation for Animal Health, formerly known as the OIE. The OIE is an international organization that sets the sanitary and health standards of animals that safeguards international trade. The OIE defines a reportable virus as "any influenza A virus of the H5 or H7 subtypes or by any AI virus with an intravenous pathogenicity index (IVPI) greater than 1.2 (or as an alternative at least 75% mortality)" (OIE, 2015). Highly pathogenic avian influenza has been known to arise from LPAI H5 or H7 subtypes, therefore making it reportable. The OIE categorizes HPAI as a List A disease. List A diseases are defined as "transmissible diseases that have the potential for very serious

and rapid spread, irrespective of national borders, that are of serious socio-economic or public health consequence and that are of major importance in the international trade of animals and animal products" (OIE, 2015). According to the Centers for Disease Control and Prevention (2015), over 700 human cases of HPAI have been reported to the World Health Organization since 2003. Countries take the threat of AI very seriously, and act accordingly. International trade of all poultry in the affected nation is shut down during an outbreak. Vaccination for HPAI can mask the disease as it only reduces the morbidity and mortality as opposed to preventing the shedding and transmission of the disease. Infected poultry or poultry products can be unknowingly traded. Therefore, controlling HPAI via vaccination has international export and trade implications (USDA-APHIS, 2015).

Even though vaccinating for HPAI can have export and trade sanctions, it can be an important tool when it comes to containing and controlling the disease (OIE, 2006). This is of particular importance in regions of the world such as South East Asia, where HPAI has become uncontrollable and endemic to the region (Eagles et al., 2009). In South East Asia, the poultry industry is far less industrialized than in the United States. Village chickens, free range duck production, live bird markets, and the uncontrolled movement of poultry are common (FAO, 2016). Biosecurity is often times very minimal and through the frequent interaction between wild and domestic birds, particularly ducks, HPAI has undergone reassortment and is now circulating in the wild bird populations (FAO, 2016).

H5N2 Outbreak of 2014-2015

The outbreak of the Highly Pathogenic Avian Influenza Virus (HPAI) in 2014-2015 was by far the largest animal disease outbreak in United States history. Genetic analysis of the virus revealed that it was a combination of an HPAI in Asia and an LPAI of American lineage. The Asian strain was most likely introduced into North America via Alaska in 2014. Birds from the two continents comingle during the summer months before migrating back south for the winter (USDA-APHIS, 2015). The fall migration brought the virus down the West Coast via the Pacific Flyway to the wintering grounds that those birds shared with birds from the Central and Mississippi Flyways. It was then spread throughout the central United States during the 2015 spring migration (USDA-APHIS, 2015).

The H5N2 virus was first detected on December 19, 2014 in a backyard poultry flock in Douglas County, Oregon (USDA-APHIS, 2015). The virus was sporadically detected on the West Coast in less than a dozen backyard and commercial chicken flocks during the months of January and February of 2015. The disease was first detected in Minnesota in Pope County on March 4, 2015 and spread rapidly thereafter. Out of 211 commercial flocks infected, 185 occurred in the upper Midwest during the months of April and May in 2015. The deadly virus was last detected on June 17, 2015 in a commercial layer flock in Wright County, Iowa (UDSA-APHIS, 2015). Within six months of its first detection, HPAI H5N2 destroyed nearly 50 million birds in 21 states, making it the largest animal disease outbreak in United States history (UDSA-APHIS,

2015). It devastated the egg laying and turkey industries in the upper Midwest and cost the government over $950 million to contain the disease.

Once an HPAI positive premise was identified/confirmed using rRT-PCR of tracheal swabs, a 3-km ‘infected zone’, a 7-km ‘buffer zone’ and a 10- km ‘control area’ perimeter was set up from the infected premise (USDA-APHIS, 2015). A USDA Incident Commander was put in charge of each infected premise. Flocks in the control area were tested daily using tracheal swabs for HPAI via PCR. Flocks outside the Control Area, but still considered to be at risk, were tested on a weekly basis. Movement within or out of a control area required a USDA permit (USDA-APHIS, 2015). This included poults, eggs, semen, feed, and any equipment. Each infected premise was to be depopulated within 24 hours of testing positive for HPAI. Due to the magnitude of the outbreak and lack of preparedness, resources and personnel were insufficient to deal with the situation. In some cases, it took days or weeks to depopulate flocks, which allowed the disease to spread even further. Once a flock was depopulated and composted properly, the premise could be cleaned and disinfected and tested. A premise could begin restocking efforts 21 days after a negative HPAI test.

Etiology

Avian influenza (AI) viruses are part of the Orthomyxoviridae family and genus Influenzavirus. It is an enveloped, spherical to pleomorphic shaped virion ranging in size from 80-120nm. The entire viral genome is enclosed in a helical nucleocapsid which

consists of eight single-stranded, negative sense, ribonucleic acid (RNA) segments (Suarez, 2008; Adam and Sandrock, 2010). The surface is covered with two types of glycoprotein projections, viral antigens; the rod-shaped trimer hemagglutinin (HA) responsible for recognizing and binding sialic acid receptors of target cells and the mushroom shaped tetramer neuraminidase (NA) that cleaves sialic acid from HA to release virons from infected cells (Vasin et al., 2014). There are 16 HA antigenic strain classifications based on haemagglutination-inhibition (HI) and 9 NA antigenic strain classifications based on neuraminidase-inhibition (NI) (Suarez, 2008).

In addition to the surface proteins, there is a membrane ion-channel protein (M2) that helps to acidify the viron and three internal proteins: the nucleoprotein (NP), the matrix protein (M1), and the polymerase complex (Vasin et al., 2014). Lastly, there are two nonstructural proteins (NS), NS1 and NS2. The NS1 protein works to evade the host's immune response by inhibiting interferon production (Krug, 2015) and suppressing Fas/Fas-ligand-mediated apoptosis (Xing et al., 2009). The NS2 protein exports the virus and regulates influenza RNA levels (Vasin et al., 2014). The NP tightly binds the RNA segments and forms the ribonucleoprotein (RNP) core (Adam and Sandrock, 2010). The M1 protein encodes the main component of the viral capsid. The polymerase complex aids in viral transcription and is composed of the polymerase basic protein 1 (PB1), polymerase basic protein 2 (PB2), and polymerase acidic protein (PA) (Vasin et al., 2014).

The virus is relatively unstable and susceptible to inactivation through heat, extreme pH, drying, organic solvents, and detergents (Saif, 2003). Organic material such as nasal secretions or feces can protect the fairly fragile virus in the environment for an extended period of time (Saif, 2003). The rate of inactivation depends on the size and composition of droplets surrounding the virus (Sooryanarain and Elankumaran, 2015). Persistence in the environmental is largely dependent upon temperature; cool-dry or cool-moist conditions favor virus survivability and transmissibility (Sooryanarain and Elankumaran, 2015). The virus was shown to survive in liquid manure for 105 days in the cool winter months (Saif, 2003).

All AI viruses are Type A influenza viruses and infect a large variety of hosts including birds, pigs, and humans. Types B and C typically do not cause diseases in poultry. Domestic fowl are not considered to be natural hosts of the virus, but typically become readily infected. Waterfowl and shore birds of the orders Anseriformes and Charadriformes are natural, asymptomatic, infectious reservoirs (Stallknecht and Brown, 2008; Cardona et al., 2009). In addition, they harbor all HA and NA viral gene combinations (Cardona et al., 2009). The virus is ubiquitous. Viral presence or anti-AI antibodies have been found on all seven continents in wild fowl (Saif, 2003). Infection in waterfowl typically results in an asymptomatic enteric infection and spreads primarily via the feces into the environment (Cardona et al., 2009). The virus can be transmitted via direct contact as well as indirect contact via aerosol droplets and contaminated fomites (Saif, 2003). Influenza viruses of low pathogenicity in wild birds can easily

mutate and reassort within the wild bird populations to produce other LPAI subtypes (Zhao el al., 2012). An HPAI typically arises from infections of LPAI of the H5 and H7 serotypes circulating in domestic fowl (Zhao el al., 2012). In particular, AI viruses of duck origin have been shown to rapidly adapt to chickens and emerge quickly (Li et al., 2009). Bird migration and air movements may contribute to environmental transmission (Sooryanarain and Elankumaran, 2015).

Once in poultry, the virus can spread rapidly via feces and nasal secretions (Swayne and Suarez, 2000) and contaminated materials (Horimoto and Kawaoka, 2005). Airborne dissemination appears to play a major role during outbreaks. Dust from wind storms during China's spring 2005 outbreak of HPAI was shown to have facilitated the spread of the disease (Liu et al., 2007). The HPAI virus can also be found in high concentrations in the semen of infected sub-clinical turkey breeder toms (Wileman, 2015). Experimental inoculations via the oviduct during insemination of the turkey breeder hen resulted in AI infections (Pantin-Jackwood et al., 2010). This potential route of transmission is of great importance to the turkey breeder industry which typically inseminates breeder hens weekly (Pantin-Jackwood et al., 2010).

The primary and most important difference between LPAI and HPAI is found in the HA cleavage sites. When the virus attaches to the sialic acid receptor of the host cell, receptor mediated endocytosis is initiated (Swayne and Pantin-Jackwood, 2008). Once inside, viral RNA is released into the cytoplasm and viral replication and assembly

within the host's cells begins. The HA precursor molecule (HA0) undergoes post-translational proteolytic cleavage via host proteases into HA1 and HA2 subunits (Horimoto and Kawaoka, 2005). The viral envelope and the endosomal membrane become fused during this process, making the virion infectious. The virus is noninfectious until cleaved. Low pathogenic avian influenza viruses possess a single arginine at the cleavage site with an amino acid sequence of RETR (Horimoto and Kawaoka, 2005). This sequence can only be cleaved by trypsin-like proteases found in the respiratory and digestive tracts (Suarez, 2008), therefore limiting the number of cells it can effectively replicate in. The HPAI viruses have cleavage sites between arginine and glycine (Post et al., 2012) and a series of basic amino acids at the cleavage site, RERRRKKR (Horimoto and Kawaoka, 2005), that can be cleaved by ubiquitous proteases found in most tissues making systemic viral replication possible (Post et al., 2012). An LPAI can be converted into an HPAI with the simple insertion of two to ten basic amino acids at the cleavage site (Post et al., 2012).

Host Defenses

Viral Sensing

The innate immune response is the bird's first line of defense against microbes. It consists of both physical and chemical barriers such as skin, tight epithelial lining of the GI tract, tears, and mucosal secretions as well as non-specific immune cells such as phagocytes and natural killer cells (Abbas et al., 2007). In birds there are two main pattern recognition receptors (PRR) that are important in recognizing viral pathogen-

associated molecular patterns (PAMPs) and activating macrophages: toll-like receptors (TLR) and retinoic acid-inducible gene I (RIG-I)-like receptors (RLR) (Chen et al., 2013). Several TLRs recognize viral PAMPs: TLR2, TLR3, TLR4, and TLR7 (Brownlie and Allan, 2011; Chen et al., 2013; Keestra et al., 2013). More importantly, TLR3 and TLR7 are key in recognizing HPAI viruses (Chen et al., 2013) and inducing antiviral responses in macrophages (Barjesteh et al., 2014). The TLRs are type-I integral transmembrane glycoprotein signaling receptors that play an important role in the innate immune response to pathogens (Chen et al., 2013; Keestra et al., 2013). They consist of three domains: the N-terminal domain which consists of leucine and cysteine rich regions, the transmembrane domain, and the intracellular Toll/IL-1 receptor domain (Brownlie and Allan, 2011). The TLRs recruit adapter proteins, protein kinases, and they activate gene transcription (Keestra et al., 2013). The activation of macrophages and subsequent downstream signaling of the PRRs leads to the expression of several innate antiviral cytokines and chemokines (Chen et al., 2013).

There are two RLRs: RIG-I and melanoma differentiation-associated gene 5 (MDA5). They contain five domains: two N-terminal caspase activation and recruitment domains, an RNA helicase domain, a C-terminal RNA-binding domain and a repressor domain (Chen et al., 2013). The RLRs are cytoplasmic sensors that bind viral RNA. They employ a signaling cascade that stimulates the expression of antiviral type-I interferons (Chen et al., 2013) to signal natural killer cells to destroy the infected cell (Abbas et al., 2007). Chickens and turkeys, unlike ducks, lack the RIG-I receptor. Both

RIG-I and MDA5 are important in sensing influenza virus in birds. The MDA5 is said to have similar functions as RIG-I (Chen et al., 2013). The interferon–induced helicase domain-containing protein 1 (IFIH1) gene encodes for MDA5.

There are two types of T-cells, CD4+ T-helper and CD8+ T- cytotoxic, that are activated via the T-cell receptor complex following virus recognition and co-stimulation (Abbas, 2007). Upon antigenic stimulation, naïve T-helper (Th) cells differentiate into subsets including T-helper 1 (Th1) and T-helper 2 (Th2) (Zhang et al., 2003). Th1 cells secrete cytokines such as IFN-γ and tend to promote cellular immunity while Th2 cells secrete another set of cytokines to down-regulate Th1 responses and support humoral immunity (Zhang et al., 2003). Viral antigen can also be presented by the MHC I associated antigen presenting cell to naïve CD8+ T-cells and assist with the lysing of infected cells. (Abbas, 2007).

Cytokines

Cytokines are peptides that are secreted to mediate cellular responses associated with the innate and adaptive immune systems (Kaiser et al. 2004). Via complex networks, these molecules send chemical signals throughout the body to initiate and control the host's response to pathogens whether it be a pro-inflammatory or anti-inflammatory reaction (Kogut, 2000). Cytokines direct the host's immune response towards cell-mediated or antibody-mediated responses by means of promoting or suppressing the proliferation of various immune cells (Kapczynski et al., 2014).

Pro-Inflammatory Cytokines

Interleukin-1β, a pro-inflammatory cytokine produced by macrophages, endothelial cells, and epithelial cells, mediates the inflammatory response of the host. The level of response or inflammation depends on the amount of IL-1β produced. Small quantities result in local inflammation. When large concentrations of IL-1β enter the blood stream, the synthesis of acute phase plasma proteins and the production of IL-6 are stimulated (Abbas et al., 2007). An increase in the production of chemokines and corticosterone can also be seen in response to elevated levels of IL-1β (Hilton et al., 2002).

Interleukin-6 is a multifunctional cytokine that is involved in hematopoiesis, immune regulation, and acute phase response (Gupta et al., 2015). As a pro-inflammatory cytokine (Kapczynski et al., 2014), it promotes the growth of B-lymphocytes (Abbas et al., 2007). It is produced by T- and B-lymphocytes, endothelial cells, fibroblasts, and monocytes (Gupta et al., 2015).

Anti-Inflammatory Cytokines

Anti-inflammatory cytokines are immuno-regulatory molecules that control the pro-inflammatory cytokine responses (Opal and DePalo, 2000). One of the most important immuno-regulatory cytokines, IL-10, is secreted by activated macrophages and T-regulatory cells (Opal and DePalo, 2000). It helps maintain the balance between the innate and cell mediated immune responses by inhibiting activated macrophages

(Abbas et al., 2007) and inflammation (Kaiser et al., 2004). Interleukin-10 is a potent IFN-γ inhibitor (Opal and DePalo, 2000). In addition to its pro-inflammatory properties previously mentioned, IL-6 has anti-inflammatory properties, inhibiting IFN-γ production (Opal and DePalo, 2000).

Chemokines

Chemokines are a large family of small cytokines that stimulate and regulate leukocyte movement from the blood into the infected tissues, also known as chemotaxis (Abbas et al., 2007). They are highly specific secondary pro-inflammatory mediators (Graves and Jiang 1995). There are two major chemokine families, CC and CXC, that are classified based on their cysteine residues (Abbas et al., 2007). The CXC family, also known as α-chemokines, have various amino acids separating the cysteine residues while the CC motif or β-cytokines do not (Graves and Jiang 1995). Chemokine are produced by numerous cell types and their secretion is triggered via TLR signaling or by inflammatory cytokines (Abbas et al., 2007). The C-C motif ligand 5 (CCL-5) is involved in mixed leukocyte recruitment. The C-X-C motif ligand 8, known as CXCLi-2 in avian species, is involved in neutrophil recruitment. This ligand was formerly termed as IL-8 (Abbas et al., 2007).

Anti-Viral Cytokines

Interferons (IFN) are multifunctional glycoproteins that are known for their anti-viral properties (Gupta et al., 2015). They are produced by white blood cells in response

to viral infections as well as virally infected somatic cells (Kogut, 2000). There are three types of IFNs but only two of which are characterized in the bird: Type I and Type II. Type I IFNs, IFN-α, are produced by virally infected monocytes and fibroblasts (Gupta et al., 2015) and are important in controlling intracellular infections (Davidson et al., 2008). IFN-γ, a Type II interferon, is produced by the T-lymphocytes and natural killer cells following stimulation (Gupta et al., 2015). IFN-γ controls the cell-mediated immune response and serves as a major activator of macrophages (Gupta et al., 2015).

The Myxovirus-resistance (Mx) and 2'5'-oligoadenylate sythetase (OAS) are IFN stimulated genes and are considered to be some of the most effective antiviral proteins produced by the host cell (Ewald et al., 2011). The Mx gene blocks viral transcription into the nucleus (Iwasaki and Pillai, 2014). The OAS family of antiviral proteins consists of four genes: OAS1, OAS2, OAS3, and OASL (Kristiansen et al., 2010). These antiviral proteins are responsible for the activation of RNase L which initiates the degradation of viral RNA in infected cells and limits viral propagation (Lee et al., 2013 and Iwasaki and Pillai, 2014). Further, OAS1 and OASL have been shown to inhibit the translation of the interferon-inducible master transcription factor of type I interferon (IRF7), thus down regulating the production of type-I interferons during viral infections and preventing tissue damage from a hyper-inflammatory response (Lee et al., 2013).

Apoptosis/Induced Cell Death

Apoptosis or induced cell death can be initiated via intrinsic or extrinsic pathways. Interaction of the death ligands, FasL (CD95L) and tumor necrosis factor (TNF) - related apoptosis-inducing ligand (TRAIL), with their specific receptor initiates the extrinsic apoptotic pathway (Ekchariyawat et al., 2011). Initiation of the pathway results in the recruitment of Fas-associated death domain containing protein (FADD) and caspase-8 to the death inducing signaling complex which then initiates the apoptosis executing caspase cascade (Ekchariyawat et al., 2011). Both TRAIL and Fas are critical in modulating lymphocyte apoptosis and immune function (Waring and Mullbacher, 1999). The H5N1 virus has been shown to evade the host's immune response by inducing the cell death of lymphocytes, dendritic cells, and monocytes thus allowing it to move beyond the respiratory tract and cause blood-borne systemic infections (Ekchariyawat et al., 2011). Specifically TRAIL has been shown to induce apoptosis of infected monocyte derived macrophages with H5N1 infections (Ekchariyawat et al., 2011). The ability of the virus to induce apoptosis of the immune cells may contribute to its pathogenesis. Activation induced cell death of the T-cells is mediated by the Fas/FasL pathway (Waring and Mullbacher, 1999). FasL is expressed on T-cells, B-cells, macrophages, and natural killer cells and its expression is upregulated with T-cell activation (Waring and Mullbacher, 1999). Blocking the expression of either TRAIL or Fas results in a significant enhancement of IFN-γ production (Zhang et al., 2003). Expression of Fas is associated mainly with Th1 cell apoptosis while the activation and

induced expression of TRAIL occurs mainly with Th2 cell apoptosis (Roberts, et al., 2003).

Cytokine and Apoptotic Response to AI

The host's cytokine response to AIs can be characterized via gene expression profiling using rRT-PCR (Kapczynski et al., 2014). Understanding, comparing, and contrasting how hosts respond to particular pathogens may pave the way to novel prevention and treatment technology. For example, asymptomatic infected individuals are not quiescent and responded immunologically very different than symptomatic individuals when experimentally infected with influenza (McClain et al., 2015). Asymptomatic individuals tend to have an early and persistent down regulation of inflammatory mediators (McClain et al., 2015). The expression of inflammatory mediators, as well as other immune related components can be accurately quantified and profiled using reverse transcribed mRNA extracted from biological samples and real time quantitative-reverse transcription-PCR (qRT-PCR) (Roth, 2002). Sequence specific primers are used to target specific genes, amplify, and then measure them (Roth, 2002). In order to calculate changes in gene expression, highly conserved endogenous housekeeping genes, commonly glyceraldehyde 3-phosphate dehydrogenase (GAPDH) are used as internal controls (Zhou et al., 2010). The cycle at which the reporter dye fluorescence increases beyond a defined threshold is known as the cycle threshold (Ct). Results are reported as actual Ct values. Changes in gene expression can be expressed as fold changes using the described $2^{-\Delta\Delta}$ Ct method (Livak and Schmittgen 2001).

Immune Evasion

Even with a highly evolved and complex immune system in the host, AI viruses are still able to evade it. Virulence can be correlated with immune evasion (Perdue, 2008; Swayne and Suarez, 2000). Avian influenza viruses use several tactics to elude the immune system. The virus is known for its high mutability and reassortment capabilities (Perdue, 2008; Swayne and Suarez, 2000). Mutating or reassorting changes the specificity of the antibody needed for host protection, thus resulting in increased viral replication and transmission of mutated strains (Hale et al., 2010). Immunoglobulin (Ig)-M is produced approximately five days post infection followed by production of IgY. The antibodies produced recognize specific subtypes of AI and do not provide cross protection (Suarez and Schultz-Cherry, 2000).

The NS viral proteins are critical in immune evasion. The NS1 protein can limit the production and effectiveness of the interferons that inhibit viral replication, (Hale et al., 2010) by blocking the cytoplasmic RIG-I/MDA5 signaling cascade or by attenuating INF-inducible signaling (Hale et al., 2010 and Vijayakumar et al., 2015). The protein can suppress the Fas/Fas-ligand-mediated apoptosis thus increasing the infectivity (Xing et al., 2009). Together with the virus polymerase complex, NS contributes to cytokine hyperinduction (Mok et al., 2009).

In general, the virus can induce and or inhibit cellular apoptosis of various cell types including immune cells (Ekchariyawat et al., 2011), increase viral replication

speed (Hale et al., 2010) and induce cytokine deregulation of the host (Kuribayashi et al., 2013). The extracellular signal-regulated kinase 1/2, which is important for viral replication, has been shown to interfere with the host's pro-inflammatory and apoptotic responses (Xing et al., 2010). Efficient viral replication, coupled with the destruction of the innate immune response, increases pathogenicity (Suzuki et al., 2009). The HPAI strain A/Turkey/Ontario/7732/66 has been shown to destroy lymphocytes both *in vitro* and *in vivo* (Suarez and Schultz-Cherry, 2000). The ability to evade the host's immune system and subsequent pathogenicity varies greatly and is highly dependent upon the individual virus (Cardona et al., 2008).

Immunopathology

Depending on the species and individual virus involved, infections with AI can be low to moderately pathogenic, with birds exhibiting sub-clinical to mild infection, to highly pathogenic and cause close to 100% mortality (Swayne and Pantin-Jackwood, 2008). Individual variation in immune response has been noted in humans and several species of birds following experimental infection (McClain et al., 2015; Hayashi et al., 2011). Specific pathological and histological lesions are highly dependent upon the individual virus itself (Cardona et al., 2008; Kuribayashi et al., 2013), the inoculum dose, and the route of exposure (Saif, 2003). For example, the HPAI A/turkey/Italy4580/1999 replicated more extensively in the brain of experimentally inoculated chickens as opposed to the chicken/Netherlands/2586/2003 H7N7 strain (Kuribayashi et al., 2013).

Cytokines are essential in clearing viral infections, but in large quantities or unregulated they can result in hypercytokinemia or "cytokine storms" and cause significant tissue damage or even death in the host (Kuribayashi et al., 2013). Cytokine storms occur when large amounts of pro-inflammatory interleukins and interferons are released into circulation as a result of the rapid proliferation and over production of highly activated T-cells and natural killer cells (Kuribayashi et al., 2013). Enhanced activation of the dendritic cells, in the chicken, following an HPAI infection may lead to the deregulation of the immune response, making the virus highly pathogenic (Vervelde, et al., 2013). Excessive levels of pro-inflammatory cytokines can trigger bleeding, clotting, and subsequent organ/tissue damage and necrosis (Kuribayashi et al., 2013). It can lead to fatal systemic capillary leakage in chickens infected with HPAI (Kuribayashi et al., 2013). IL-1β and Il-6 are believed to be partially responsible for the induced pathology in infections with AI (Burggraaf et al., 2014).

Clinical signs are often times a result of viral replication and consequent tissue damage to the visceral organs and the cardiovascular and nervous systems (Saif, 2003). Tissue damage can be caused by actual virus replication or cytokine production (Saif, 2003). High mortality prior to the onset of clinical signs can be seen with HPAIs due to its ability to replicate rapidly and to quickly become systemic (Saif, 2003). Although there is variability with regards to site and extent of the lesions between strains of HPAI (Mo et al., 1997), the most prevalent histological lesions associated with HPAIs are multi-organ necrosis and inflammation of the brain, heart, pancreas, and lymphoid

organs (Saif, 2003). The virus quickly attacks both the vascular endothelial cells and perivascular tissue cells leading to swelling of the microvascular endothelium, systemic congestion, perivascular mononuclear cell infiltration, multifocal hemorrhages, and thrombosis (Kobayashi et al., 2007). Lesions are typically associated with viral antigen presence in the cells. In severe cases of HPAI, viral antigen can be found in tissues in the absence of lesions (Hagag et al., 2015). Virus can be found in multiple organs following infections with HPAIs including the lung (Hayashi et al., 2011; Mo et al., 1997), kidney (Hayashi et al., 2011; Mo et al., 1997), pancreas (Mo et al., 1997), spleen, liver (Hayashi et al., 2011), cardiac myocytes (Kobayashi et al., 2007), and in the neuron and glial cells of the brain (Hayashi et al., 2011). Viral antigen was detected between the seminiferous tubules and on the heads of the sperm inside in naturally infected chickens (Hagag et al., 2015). Rapid virus replication in the macrophages and vascular endothelial cells leads to the destruction of thermoregulation and the innate immune system (Suzuki et al., 2009).

Ducks

In general, ducks are typically asymptomatic and have a very strong antiviral response and weak/moderate pro-inflammatory response to infections with AI viruses (Adams et al., 2009). Ducks exhibit a down regulation of MHC II resulting in a less robust antibody response (Adams et al., 2009) and subsequently the lowest antibody titer when compared to other species challenged with AI (Suarez and Schultz-Cherry, 2000). The PRR RIG-I response is present in the duck. It detects RNA ligands derived from uncapped viral transcripts and initiates antiviral pathways. Expression of RIG-I has been

shown to increase as much as 200 fold when challenged with H5N1, thus linking RIG-I to the early antiviral innate immune response (Barber et al., 2010). Additionally, TLR3 is down-regulated in the lungs of the duck when challenged with HPAI (Chen et al., 2013). Ducks express a very different pattern of the interferon-induced transmembrane protein (IFITM) genes and cytokines when compared to the chicken (Smith et al., 2015). There is a marked decrease in the production of interferons and a strong up regulation of IFITM 1, 2, and 3 as well as anti-inflammatory cytokines in ducks infected with HPAI. Recently, the importance of the IFITM-3 and its antiviral activity against AI viruses in the duck (Blyth et al., 2016) were described, further reiterating its significance in AI infections. Furthermore, ducks exhibit a slow induction of IL-6 and the acute phase protein serum amyloid A compared to the rapid upregulation in chickens (Burggraaf et al., 2014). Inoculated duck lung cells showed little change in the signal transducer and activator of transcription-3 (Kuchipudi et al., 2014).

Another unique host mechanism, and potential protective strategy, is the ability of infected cells to undergo rapid death thus limiting viral replication (Kuchipudi et al., 2012). Duck cells experimentally infected with a HPAI H5N1, that was non-fatal to ducks, underwent rapid cell death as opposed to a very slow cell death observed with the Eurasian H5N2 known to be fatal (Kuchipudi et al., 2012). Rapid apoptosis of infected cells typically occurs before viral replication and assembly are completed, thus limiting its replication. The dead cells then undergo subsequent phagocytosis and the virus is

cleared from the host (Kuchipudi et al., 2012). This mechanism has not been described in other species.

Chickens

Chickens appear to have a rapid, systemic, and often fatal reaction following infections with HPAIs that typically consist of high viral loads, extensive tissue damage, and an intense activation of the innate immune response (Burggraaf et al., 2014). High pro-inflammatory cytokine levels tend to coincide with the presence of lesions in chickens (Adams et al., 2009). Chickens also tend to produce very high antibody titers in response to an infection (Suarez and Schultz-Cherry, 2000). The PRR RIG-I is absent in the chicken and believed to partially explain the increased susceptibility to infection (Barber et al., 2010). Chickens appear to have very little IFITM response as well when compared to ducks (Smith et al., 2015). Susceptibility also appears to have a genetic component. Some variants of the Mx gene do not produce antiviral activity whereas other variants do. Chickens expressing the Asn631 allele of the Mx proteins had increased antiviral activity and were more resistant to infection than those expressing the Ser631 allele that does not encode for antiviral activity (Ewald et al., 2011).

Experimental studies in the chicken regarding viral replication and subsequent innate immune response have contributed to the overall understanding of AIs. Although wide ranges of cytokine response has been reported (Adams et al., 2009), trends have developed. Intranasally inoculated chickens with HPAI H7N1 induced a significant

increase in IFN-γ, IL-1β, IL-6, and IFN-α in proportion to the virus proliferation in the brain, lungs, heart, kidney, spleen, and colon (Kuribayashi et al., 2013). Early death in chickens infected with HPAI H5N1 was associated with the upregulation of IFN-α, IFN-γ, and Mx1 as well as increased viral replication in the lungs and spleens (Wasilenko et al., 2009). A significant increase in CXCLi-2, IFN-α, IFN-γ, TLR1, TRL3 and TLR-21 following experimental challenge of chickens with HPAI H7N2 and H5N2 has been demonstrated (Vervelde et al., in 2013).). Strong induction of IL-6, IL-12, and IFNs are found in the lung and spleen of chickens infected with HPAI H5N1 (Vervelde et al., in 2013). Levels produced were dependent upon viral strains (Vervelde et al., in 2013). The signal transducer and activator of transcription (STAT)-3, which is responsible for mediating the pro-inflammatory response, was found to be down-regulated and IL-6, CXCLi-2, and IL-10 were highly upregulated in chickens lung cells experimentally infected with HPAI H5N1 (Kuchipudi et al., 2014).

There have been large differences in viral RNA concentrations and host gene expression noted between chickens infected with HPAI or LPAI in the brain (Post, et al., 2012). Viral RNA can be found throughout the body but replication in the brain and subsequent apoptosis of the HPAI infected brain cells appears to be the most remarkable differences between HPAI and LPAI in chickens (Post, et al., 2012). Viral RNA and antigen were detected in all tissues in naturally infected broilers with HPAI H5N1 in Egypt, with the highest levels seen in the brain and trachea (Hagag, et al., 2015).

Excessive cytokine response has led to fatal systemic capillary leakage particularly in the brain of chickens infected HPAIs (Kuribayashi et al., 2013).

There is only one document which examines the reproductive tract response of egg laying hens infected with AI, however it is with an LPAI. Hens experimentally infected with H9N2 resulted in significant tissue damage and apoptosis in all segments of the oviduct (Wang et al., 2015). In addition, gene expression of TLR3, MDA5, IL-2, IFN-β, CXCLi1, CXCLi2, XCL1, XCR1, and CCR5 were shown to fluctuate across regions and throughout the course of the infection (Wang et al., 2015). It is unknown if this response is similar to the infection seen with HPAIs.

Pigeons

Following the experimental inoculation of pigeons with HPAI H5N1, viral RNA was recovered from the lungs, spleen, brain, liver, kidneys, and rectum of the birds (Hayashi et al., 2011). Lesions were occasionally produced in the brain but varied by individual and ranged from no observable lesions to severe encephalitis (Hayashi et al., 2011). Viral load in the brains was correlated with the level of IL-6 and IL-1B expression in the brain (Hayashi et al., 2011).

Turkeys

While the host's immune response to avian influenza has been described in mammals and to an extent in the chicken and duck (Blyth et al., 2016; Cardona et al.,

2008; Kuchipudi et al., 2012; and Swayne, 2008), there are less than a handful of articles documenting the immune response in the turkey. All of which describe experimental inoculations with LPAIs and have been published within the last three years (Mondal et al., 2013; Umar et al., 2015; Umar et al., 2016). Virus has been shown to be recovered from the blood and muscle of turkeys experimentally infected with HPAI H7N1 (Toffan et al., 2008). But with this particular virus, all birds were dead or clinically sick within 2 days post infection, unlike what was seen with the current study. In addition, there is evidence indicating that the turkey's immune response is not comparable the chickens'. The HPAI H5N2 virus involved in the 2015-2016 outbreak was shown to have reduced adaptation and transmissibility in the chicken when compared to the turkey (Bertran, et al., 2016). Based on this information, one can conclude that the chicken and the turkey responded differently to the exact same virus. This would not be the first time that the turkey was known to respond differently to the same pathogen and lead to increased pathogenesis (Powell et al., 2009). Furthermore, there is greater divergence at the proteome level between the chicken and turkey than there is between humans and chimpanzees (Arsenault et al., 2014), offering additional proof that the immune system of these two avian species are substantially different.

There are no documented cases of HPAI in wild turkeys, despite the massive outbreaks in the domestic populations. When compared to their wild counterparts, the modern domestic turkey has shown to have decreased heterophil function (Genovese et al., 2006) as well as reduced or inefficient TLR signal transduction which are important

in detecting and protecting against viruses (Genovese et al., 2007). The potential influence the inferior immune response of the domestic turkey has on HPAI pathogenesis has yet to be elucidated. Viral pathogenesis and interactions with the host response with regards to HPAI in turkeys is mainly unidentified.

Information regarding experimentally infected turkeys with HPAIs is novel and minimal and information detailing the response of naturally infected turkeys does not exist. Field data from naturally infected turkeys is essential for describing and understanding the dynamics of the disease during an outbreak. A better understanding of the host's immune response, as well as the characteristics of the virus under field conditions may offer insight into better controlling strategies or options to controlling the disease without impacting international trade (USDA-APHIS, 2015).

CHAPTER II

VIRAL DISTRIBUTION, SEMI-QUANTITATIVE VIRAL LOAD IN THE TISSUES, AND QUALITATIVE TISSUE ANALYSIS

Overview

The outbreak of the highly pathogenic avian influenza virus (HPAI) in 2014-2015 was by far the largest animal disease outbreak in United States history. The outbreak crippled both the turkey and egg laying industries. Up to that point, minimal research had been done regarding HPAIs in the turkey. This study examined viral distribution, semi-quantitative viral load, and histological viral lesions in 8 tissues from clinical, sub-clinical, and negative control birds: brain, heart, GI, liver, lung, reproductive tract, spleen, and trachea. The matrix gene was detected in all 8 of the tissues in the clinical and sub-clinical groups. The clinically affected birds had significantly lower Ct values, or higher matrix gene content, in the brain, GI, spleen, and trachea than the sub-clinically affected turkeys.

Interestingly, with the massive mortality associated with this outbreak, histological viral lesions were in general very mild and insignificant. The majority of the histological changes were confined to the trachea and liver in the clinically positive birds and primarily consisted of the infiltration of small numbers to heterophils, lymphocytes, and macrophages. In addition to the changes seen in the trachea and livers, the sub-

clinical birds displayed more birds with infiltration of heterophils, lymphocytes, and macrophages in the oviduct and heart.

Introduction

Avian influenza (AI) viruses are part of the Orthomyxoviridae family and genus Influenzavirus (Suarez, 2008). The entire viral genome consists of eight single-stranded, negative sense, RNA segments (Perdue, 2008; Adam and Sandrock, 2010). The surface of the virion is covered with two types of glycoprotein projections; hemagglutinin (HA) and neuraminidase (NA) (Vasin et al., 2014). There are 16 HA antigenic strain classifications based on haemagglutination-inhibition (HI) and 9 NA antigenic strain classifications based on neuraminidase-inhibition (NI) (Stallknecht and Brown, 2008).

All AI viruses are Type A influenza viruses and infect a large variety of hosts including birds, pigs, and humans. Domestic fowl are not considered to be natural hosts of the virus, but typically become readily infected. Waterfowl and shore birds of the orders Anseriformes and Charadriformes are natural, asymptomatic, infectious reservoirs (Swayne and Pantin-Jackwood, 2008; Cardona et al., 2009). An HPAI typically arises from infections of LPAI of the H5 and H7 serotypes circulating in domestic fowl (Zhao el al., 2012). The HA LPAI viruses can only be cleaved by trypsin-like proteases found in the respiratory and digestive tracts (Horimoto and Kawaoka, 2005 and Suarez, 2008). In contrast, the HA of HPAI viruses can be cleaved by ubiquitous proteases found in

most tissues, making systemic viral replication possible (Horimoto and Kawaoka, 2005 and Post et al., 2012).

While the HPAI virus and host interaction has been described to an extent in the chicken and duck (Blyth et al., 2016; Cardona et al., 2008; Kuchipudi et al., 2012; and Swayne, 2008), published literature regarding HPAIs and the turkey is scarce. Virus has been recovered from the blood and muscle of turkeys experimentally infected with HPAI H7N1 (Toffan et al., 2008) but virus characteristics and host susceptibility were very different than what would occur with a different virus and under natural field conditions. It is also unknown if what has been previously seen in the chicken is applicable to the turkey as there is greater divergence in the proteome level between the chicken and turkey than initially thought (Arsenault et al., 2014). The HPAI H5N2 virus involved in the 2014-2015 outbreak was shown to have reduced adaptation and transmissibility in the chicken when compared to the turkey (data pending pub.). Furthermore, nearly 70% of cases reported during the outbreak involved turkeys (USDA-APHIS, 2015). Based on this information, one can conclude that the chicken and the turkey responded differently to the exact same virus. This would not be the first time that the turkey was known to respond differently to the same pathogen and lead to increased pathogenesis (Powell et al., 2009).

H5N2 Outbreak of 2014-2015

The outbreak of the Highly Pathogenic Avian Influenza Virus (HPAI) in 2014-2015 was by far the largest animal disease outbreak in United States history. Within six months of its first detection, HPAI H5N2 destroyed nearly 50 million birds in 21 states, making it the largest animal disease outbreak in United States history (UDSA-APHIS, 2015). It devastated the egg laying and turkey industries in the upper Midwest and cost the government over $950 million to stop the disease.

This study examined the viral distribution and semi-quantification of the matrix gene in the brain, heart, GI, lung, liver, reproductive tract, spleen and trachea of turkey breeder hens. Tissues were further categorized by clinical or sub-clinical bird status. Histopathology was also conducted on all of the tissues. This is the first study of its kind that characterizes the 2014-2015 HPAI H5N2 virus in naturally infected turkey breeder hens with regards to viral distribution and semi-quantitative viral loads in addition to describing histological lesions. This information enhances the general understanding and properties of the virus and the histological changes in the turkey during the spring 2015 outbreak of HPAI H5N2. In general, information regarding HPAIs in experimentally infected turkeys is minimal and information detailing the response of naturally infected turkeys does not exist. Field data from naturally infected turkeys is essential for describing and understanding the dynamics of the disease during an outbreak.

Materials and Methods

Experimental Birds/Tissue Collection

Breeder flocks used in the trial were both located on an AgForte (Willmar, MN) Independent Egg Producer's (IEP) farm. Each flock was comprised of Hybrid Converter turkey breeder hens approximately in the 28th week of egg production. The layout of the two sites was similar. Each farm had two laying hen barns that were connected by a central corridor with an egg washer and egg cooler. Farm management was similar between the farms. Birds were hatched and then brooded and grown together on their respective farms, prior to being divided into their respective lay barns. The positive flock used for the trial was located near Belgrade, MN. The site housed approximately 7,000 breeder hens, which were divided between Barn-1 and Barn-2. The flock was sampled in April during the outbreak of HPAI H5N2 in Minnesota. The negative control flock of was located near Benson, MN. The Benson flock consisted of approximately 10,000 birds turkey breeder hens, split between two barns, in their 28th week of production. The flock was sampled in October when the HPAI outbreak was over. Every effort was made to find an appropriate negative control flock, however due to the spread of HPAI in breeder turkeys none were found during the outbreak time period.

Collection of Tissues from Infected Birds during HPAI H5N2 Outbreak

The positive flock was in an HPAI control zone and identified and chosen via active flock surveillance in accordance with the USDA's HPAI Response Plan. On April 23, 2015 tracheal swabs from Barn-1 were suspect for HPAI H5N2 based on qRT-PCR

with a Ct value of 36.27. On April 24, Barn-1 tested positive with a Ct value of 20.92. Cycle threshold values greater than 40 were considered negative, 35-40 were suspect, and values less than 35 were positive.

On April 25, one day after the barn tested positive, ten clinically affected hens, nearing death, were randomly selected for the study. Tracheal swabs were taken and then pooled to five samples per tube in brain heart infusion (BHI) tubes. Birds were then humanly euthanized according to Ag Forte's animal welfare guidelines via cervical dislocation with a Koechner® euthanasia device (Tipton, MO). An approximately one cm^3 section of the heart, liver, spleen, trachea, lung, intestine (adjacent to the Meckel's diverticulum), oviduct (magnum), and forebrain were collected and placed into a bottle containing 35 mL of 10% neutral buffered formalin (Fisher Scientific, Fremont, CA). Tissues from each bird were pooled in individual containers and labeled. An approximate 0.5 g piece of the adjacent tissue was taken from the previously mentioned tissues and placed in 0.5 mL of RNAlater® (Qiagen®, Valencia, CA). The trachea and intestinal tract were rinsed with sterile saline prior to being placed in the RNAlater®. Tissues were held for 24 hours at 4 °C and then stored at -80 °C.

Due to the rapid spread of HPAI and a bottleneck on resources and depopulation crews, it took anywhere from days to weeks to depopulate infected premises. According to the HPAI Rapid Response Plan, the goal is to depopulate the flock within 24 hours of testing positive (USDA-APHIS 2015). Therefore 3 days later, 10 "non-clinical" birds

were randomly selected. The birds were euthanized and tissues were collected as previously described.

Collection of Tissues from Negative Control Birds

One of the pooled tracheal samples taken from the proposed control birds in Barn-2 at the Belgrade farm tested suspect on day of collection with a Ct value of 38.69. Therefore, 4 months after the last detected case of H5N2, a flock of comparable genetics, weeks in lay, and management style as the positive flock was identified to serve as the negative control baseline. Ten normal hens from one barn were randomly chosen for the study. To ensure that the birds were AI negative, tracheal swabs were taken and pooled in BHI at five samples per tube. Hens were euthanized and tissues were collected in the same manner as previously described.

RNA Extraction

RNA extraction was completed at the University of Minnesota's Mid-Central Research and Outreach Center in Willmar, MN. Four birds from each of the groups, a total of 12 birds per tissue, were selected for RNA extraction. The RNA was extracted from the tissues using an RNeasy® Mini Kit (Qiagen) and prefilled 2 mL tubes containing MagNA® Lyser Green Beads (Roche Life Science®, Indianapolis, IN). Prior to starting, 600 µL of Buffer RLT and β-mercaptoethanol (β-ME) (Qiagen), mixed at a rate of 1 µL β-ME to 1 mL Buffer RLT, was added to each MagNA® Lyser tubes. Approximately 30 mg of tissue was placed in the MagNA® Lyser Green Bead tubes and

homogenized using a MagNA® Lyser instrument at 8000 x g for 90 seconds. MagNA® Lyser Green Bead tubes were then centrifuged at maximum speed for 3 minutes. Next, 350 µL of the supernatant was pipetted into a new 2 mL microcentrifuge tube along with 350 µL of 70% ethanol and thoroughly mixed via a pipette. The solution was transferred to an RNeasy® spin column and centrifuged at 8000 x g speed for 30 seconds. The flow-through was discarded. Then, 700 µL of RW1 Buffer (Qiagen) was added to the column and the column was spun at 8000 x g for 30 seconds. The flow through was again discarded. Next, 500 µL of RPE Buffer (Qiagen) was added to the column and spun for 30 seconds at 8000 x g. The flow-through was discarded and an additional 500 µL of RPE Buffer was added to the column and spun for 2 minutes. The column was then transferred into a new 2 mL collection tube and spun at maximum speed for 1 minute. The column was then transferred into a 1.5 mL collection tube and 50 µL of RNase free water (Qiagen) was added. The column was spun at 8000 x g for 1 minute and the RNA eluate was aliquoted into 4, 10 µL samples, and stored at -80 °C.

Histological Preparation

The tissues for histological examination were prepared and processed by the University of Missouri in Columbia, MO. After fixation, the tissues were dehydrated in varying concentrations of alcohol ranging from 30-90%. Tissues were then trimmed and embedded in Paraplast® (Leica Biosystems®, Buffalo Grove, IL) for cross sectioning. A 5 µm transverse slice was sectioned, placed on a microscope slide, and stained with hematoxylin-eosin. All tissues from all birds collected were examined for histological

changes. Tissues were compared to the control group and significant histological changes reported.

Viral Detection and Semi-Quantification in the Tissues

Viral detection and semi-quantification was carried out by technicians at the University of Minnesota's Mid-Central Research and Outreach Center. Previously extracted RNA, matching those samples that were in the cytokine analysis, was used for this process: 3 clinical, 3 non-clinical, and 2 negative controls. To ensure the quality and quantity of the RNA was preserved, it was reassessed using a NanoDrop® spectrophotometer. All RNA samples were standardized to 12 µL with RNase-free water to contain 500 ng/µL. The PCR tests were set up and carried out using an AgPath® One step RT-PCR kit (Life Technologies, Grand Island, NY). The RT-PCR master mix was prepared as follows for each reaction: 12.5 µL of 2× master mix, 1 µL of enzyme mix, 1.6 µl detection enhancer, 0.5 µL of the M+25 forward primer, 0.5 µL of the M-124 reverse primer, 0.5 µL of the M-124SIV reverse modified primer, 0.5 µl of M+64 Probe, and 0.5 µl of RNase inhibitor. Next, 8 µl of RNA was then added to each reaction. Negative and positive controls were used with the reaction. The procedure, probes, and primers used have been validated by the USDA for the detection of Type A influenzas (Spackman, 2014) (Table 1. Primers and Probes)

Matrix Gene Primer/Probes	Sequence (5'-3')
M+25 Forward Primer	AGA TGA GTC TTC TAA CCG AGG TCG
M+64 Probe	56-FAM/TC AGG CCC CCT CAA AGC CGA /36-TAMSp
M-124 Reverse Primer	TGC AAA AAC ATC TTC AAG TCT CTG
M-124SIV (Reverse Modified Primer)	TGC AAA GAC ACT TTC CAG TCT CTG

Table 1. Probe and primer sequences used for the matrix gene.

The PCR analysis was then run on an Applied Biosystems® 7500 Real-Time PCR System. See Table 2 for cycling conditions. Melting curves and amplification plots were analyzed for specificity.

Step	Stage	Reps	Temp	Time
Reverse Transcription	1	1	45ºC	10 min
RT Denaturation	2	1	95ºC	10 min
Amplification	3	45	94ºC 60ºC	15 sec 45 sec

Table 2. PCR cycling conditions used in the matrix gene analysis.

Statistical Analysis

Results were expressed as Ct values. A Student's T-test was conducted on all Ct values using JMP® Pro 12 software. Probability (p)-values <0.05 were considered statistically significant.

Results and Discussion

Tissue Collection

Based on active surveillance, it is presumed that the flock was exposed on April 23, 2015, when viral RNA was first detected at a very low level in the barn. On April 24, 2015, the day the flock officially tested positive, mortality and clinical signs in Barn-1 were minimal; less than a dozen turkeys died and activity was only slightly depressed from normal. On April 25, one day after the barn tested positive, mortality was roughly 40% by mid-morning and increasing rapidly and the barn was unusually quiet with minimal bird activity (Figure 3). Birds were weak and feverish to the touch. Some birds stood in a hunched position with their heads hanging down while others sat on their hocks in a comatose state with their pupils fully dilated and irises a very pale gray color as opposed to the normal blue (Figures 4, 5, and 6). Ruffled feathers, paralysis and incoordination have been reported previously in chickens infected with HPAI (Spickler et al., 2008) but other respiratory symptoms sometimes associated with infected chickens was not seen.

Figure 1. Flock behavior.

Figure 2. Typical bird stance.

Figure 3. Image of the eye with dialated pupil.

Figure 4. Image of the eye.

Cloudy and fibrinous pericardial sacs, hemorrhaging on the spleen, and regression of the oviducts of varying degrees were noted upon necropsy in a few of the birds (Figures 7 and 8). Besides the regression of the oviduct, the majority of the birds did not have any observable lesions upon necropsy. Three days after the barn tested positive, on April 27, mortality was approximately 90%. Approximately 5% of the flock survived and appeared to be “unaffected” or “non-clinical” (Figures 9 and 10). They were active, alert, and not feverish. Necropsy lesions were minimal and similar to those seen with the clinical birds.

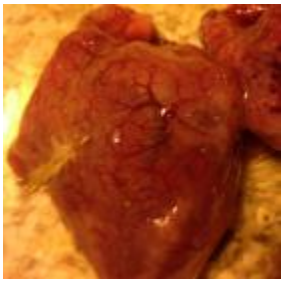

Figure 5. Example of heart lesions.

Figure 6. Example of spleen lesions.

Figure 7. Non-clinical bird.

Figure 8. Another non-clinical bird example.

Virus Distribution

Virus was found in all of the eight tissues collected from the clinical and non-clinical birds: brain, GI, heart, liver, lung, reproductive tract, spleen, and trachea. The matrix gene was not detected in any of the negative control tissues. The clinical birds had significantly lower Ct values in the brain, GI, spleen, and trachea than the non-clinical indicating the increased presence of virus in those tissues. See Figure 11 and Table 3.

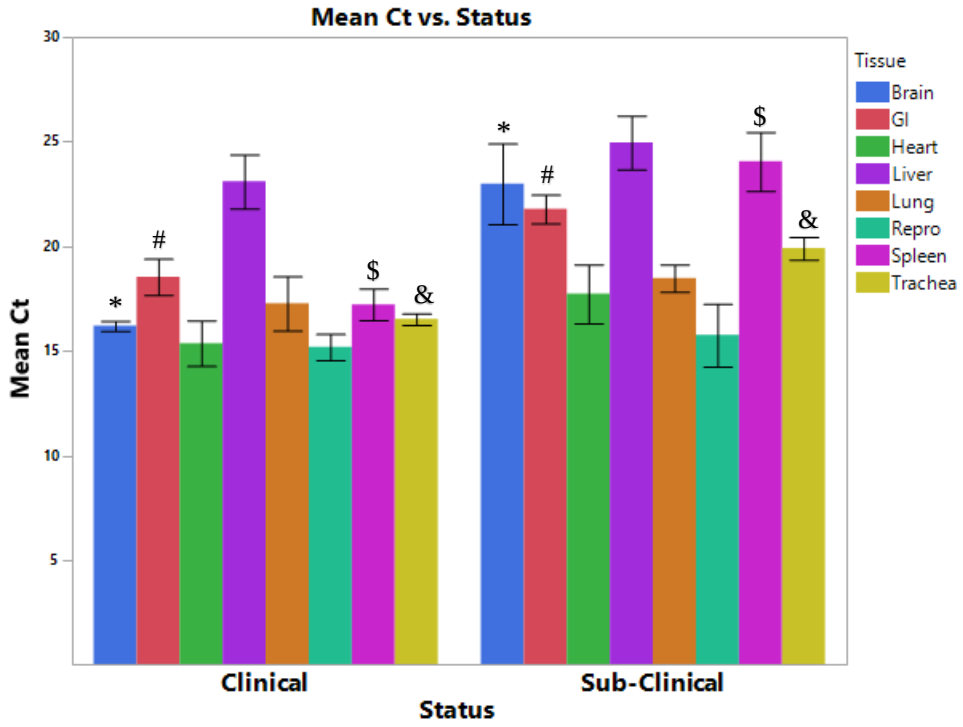

Figure 9. Mean Ct values with standard error bars for positive tissues by clinical and sub-clinical status. Statistical analysis of tissues comparing clinical and sub-clinical status. Tissues with the same symbol indicate that Ct values for that particular tissue are statistically different from each other. N=48.P-values <0.05 were considered significant.

Tissue	Clinical Mean Ct	Standard Error	Sub-Clinical Mean Ct	Standard Error
Brain	16.23	0.24	23.00	1.93
GI	18.56	0.86	21.80	0.68
Heart	15.4	1.08	17.75	1.40
Liver	23.11	1.29	24.97	1.28
Lung	17.30	1.30	18.50	0.65
Repro	15.21	0.63	15.78	1.49
Spleen	17.24	0.75	24.07	1.41
Trachea	16.55	0.27	19.93	0.54

Table 3. Mean Ct values with standard error for positive tissues by clinical and sub-clinical status.

When considering all of the tissues from all birds, the sub-clinical birds had significantly higher Ct values compared to the clinical birds, 20.73 with a standard error of 0.74 and 17.45 with a standard error of 0.56 respectively, indicating less virus present in the tissues overall of the non-clinical birds. (Figure 12). Of all positive tissues, the reproductive tracts, heart, lung, and trachea tended to have the lowest Ct values. The reproductive tract had significantly lower Ct values than all other tissues on the contrary the liver had significantly higher Ct values than all other tissues (Figure 13). Among the clinical birds, the reproductive tract and the heart had the most virus while the liver and the GI had the least. The hearts and reproductive tracts contained the most virus in the non-clinical birds while the liver and spleen had the least. (Figures 14 and 15).

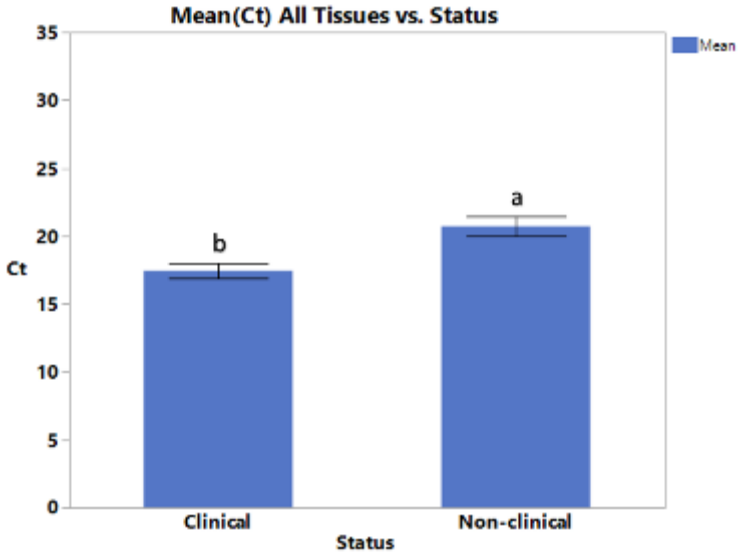

Figure 10. Mean Ct of all tissues combined by clinical and non-clinical status. N=48. P-values <0.05 are statistically significant.

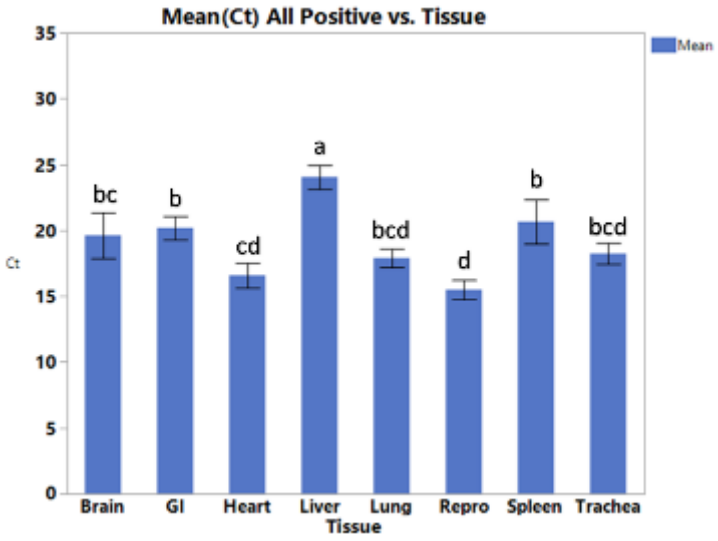

Tissue	Mean Ct	Standard Error
Liver	24.04	0.91
Spleen	20.66	1.68
GI	20.18	0.88
Brain	19.61	1.75
Trachea	18.24	0.80
Lung	17.90	0.70
Heart	16.58	0.95
Repro	15.50	0.74

Figure 11. Mean Ct and analysis of tissues of all positive birds regardless of clinical status. N=48. P-values <0.05 are statistically significant.

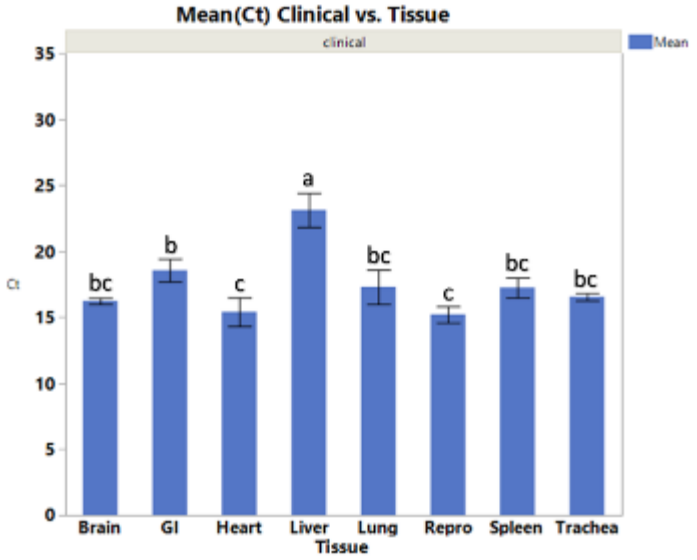

Figure 12. Mean Ct and analysis of tissues among clinical birds by. N=24. P-values <0.05 are statistically significant.

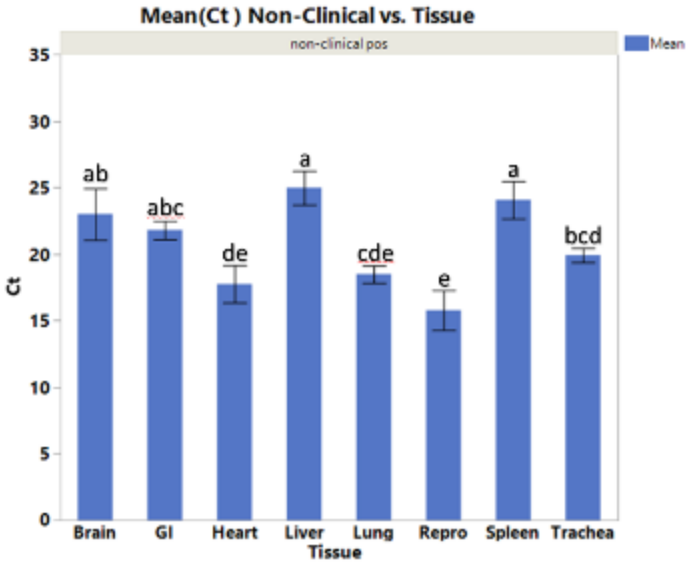

Figure 13. Mean Ct and analysis of tissues among non-clinical birds. N=24. P-values <0.05 are statistically significant.

Based on the detection of the matrix gene using rRT-PCR, virus was detected in the tissues of all birds collected from the HPAI affected barn, regardless if the bird was clinical or sub-clinical. The virus was found in multiple tissues throughout the body, which is consistent with what has been previously reported with HPAI infections in other species of birds including the chicken and the pigeon. The virus has been reported in the blood and muscle of turkeys infected with HPAIs (Toffan et al., 2008), but its presence in the other tissues was not previously described. Not only does this current study show that the virus can be found in the brain, heart, GI, liver, lung, reproductive tract, spleen, and trachea, but it is found in significantly different amounts in the tissues. The reproductive tract, heart, and lung had the lowest Ct values among the positive birds indicating that the virus was able to replicate more rapidly in those tissues. This is consistent with the lesions that were observed upon necropsy.

There is also a significant difference in the amount of virus found in the tissue of clinical *versus* sub-clinical birds. The clinical birds had the lowest Cts and highest Matrix gene detection in the reproductive tract, followed by the heart, brain, trachea, spleen, lung, GI, and liver. The sub-clinical birds had a somewhat different Ct profile. The sub-clinical birds also had the lowest Cts and highest Matrix gene detection in the reproductive tract, followed by the heart but the differed thereafter. The heart was followed by the lung, trachea, GI, brain, spleen, and liver. The sub-clinical birds had significantly higher Ct values in the brain, GI, spleen, and trachea than the clinical birds. The largest Ct differences between groups was with the spleen and the brain, 6.83 and

6.77 respectively. The lower Ct values in the clinical birds, particularly in the brain, is likely responsible for the comatose like behavior, pale irises, and dilated pupils seen prior to tissue collection. The ability of HPAI to replicate in the brain was shown to set it apart from the LPAI (Post et al., 2012). The higher levels of virus in the brain may explain the clinical signs. The differences seen in matrix gene levels and subsequent Ct values provide further insight into differences between clinical and sub-clinical birds.

Histology

Historically, there is variability with regards to site and extent of the lesions between strains of HPAI (Mo et al., 1997). The most common histological lesions associated with HPAIs are multi-organ necrosis and inflammation of the brain, heart, pancreas, and lymphoid organs (Saif, 2003) as well as swelling of the microvascular endothelium, systemic congestion, perivascular mononuclear cell infiltration, multifocal hemorrhages, and thrombosis (Kobayashi et al., 2007). None of this was seen with the current trial.

There were a variety of lesions seen in the clinically positive birds, the most predominant being in the trachea and liver. In general, the histological lesions were mild. In 6/10 birds, the mucosal lining of the trachea was infiltrated by small numbers of lymphocytes and macrophages (Figure 16). In addition, many epithelial cells in the mucosal lining were vacuolated in one bird. See Figure 17. Out of the clinical birds examined, 8/10 had various parts of the liver infiltrated by small numbers of heterophils,

lymphocytes and macrophages. Two of the birds had lesions in the oviduct: one bird had a few clumps of heterophils, macrophages, and fibrin adhered to the serosa of the oviduct, the oviduct of the other bird contained proteinaceous fluid and degenerated heterophils in the lumen. One bird had a few lymphoid nodules in the lamina propria of the intestine and another had multiple foci in the spleen in which the sinusoids contained fibrin (Figure 18).

The sub-clinical birds had a few similar lesions but a few very different ones as well. Similarly, they had trachea and liver lesions; 6/10 birds had small numbers of lymphocytes and macrophages infiltrating the mucosal lining of the trachea. 5/10 birds had infiltration of a small to moderate number of macrophages, lymphocytes, and heterophils in the various sections of the liver (Figure 19). The sub-clinical birds had lesions in the oviduct as well: 4/10 had small numbers of heterophils, lymphocytes, and macrophages infiltrating the lamina propria or serosal lining of the oviduct (Figure 20). Unlike the clinical birds, birds from the non-clinical group had heart and brain lesions. There were 3/10 birds with heart lesions: one of them had a moderate number of macrophages, lymphocytes, and heterophils infiltrating the epicardium, and two birds had a thick layer of fibrin and degenerated inflammatory cells covering the epicardium (Figure 21). Only one bird exhibited lesions of the brain. The medium-sized blood vessels of the brain were cuffed by small numbers lymphocytes and there were a few foci of necrosis in the white matter that were infiltrated by small numbers of macrophages and lymphocytes. See Figure 22. The additional lesions seen in the sub-

clinical birds may be from a different or more protective immune response or simply from being sacrificed/infected 2 days longer than the clinical birds.

The lack of significant histological lesions, despite viral presence, is not surprising, as similar results have been seen with certain HPAIs previously in chickens. The majority of the histological changes were confined to the trachea and liver in the clinically affected birds and primarily consisted of the infiltration of small numbers of heterophils, lymphocytes, and macrophages. The sub-clinical birds also saw in increase in infiltration of the heterophils, lymphocytes, and macrophages in the oviduct and heart. The increased infiltration of immune cells in the tissues of the sub-clinically affected, may potentially indicate a more protective host response. The presence of the virus in the brain, not only in the current study but also in previous studies, has led to the question as to how the virus penetrates the blood/brain barrier. It has been speculated that is comes directly through the bloodstream. The cuffing of the medium sized blood vessels with lymphocytes supports that hypothesis.

Lesions are often times a result of viral replication and consequent tissue damage to the visceral organs (Saif, 2003). This was not the case in the current study, as virus was detected in the absence of tissue damage. The virus has been shown to inhibit cellular apoptosis of various cells (Ekchariyawat et al., 2011) and the lack of apoptosis in the tissues, despite presence of the virus, indicates this may have been occurring. The lack of histological lesions is interesting but not surprising given the very rapid onset of

mortality. The increased infiltration of immune cells in the tissues of the sub-clinically affected birds may indicate a superior or more efficient immune response. Based on the histological analysis, it is very obvious that organ necrosis was not killing the birds. The results then indicate that another factor, other than multi-organ necrosis, such as hypercytokinemia or cytokine storm may be responsible for the deadly outcome. Immunohistochemistry on all tissues is currently being pursued. Being able to pinpoint and describe the exact location of the virus in the tissues will provide further insight into its cellular distribution and replication.

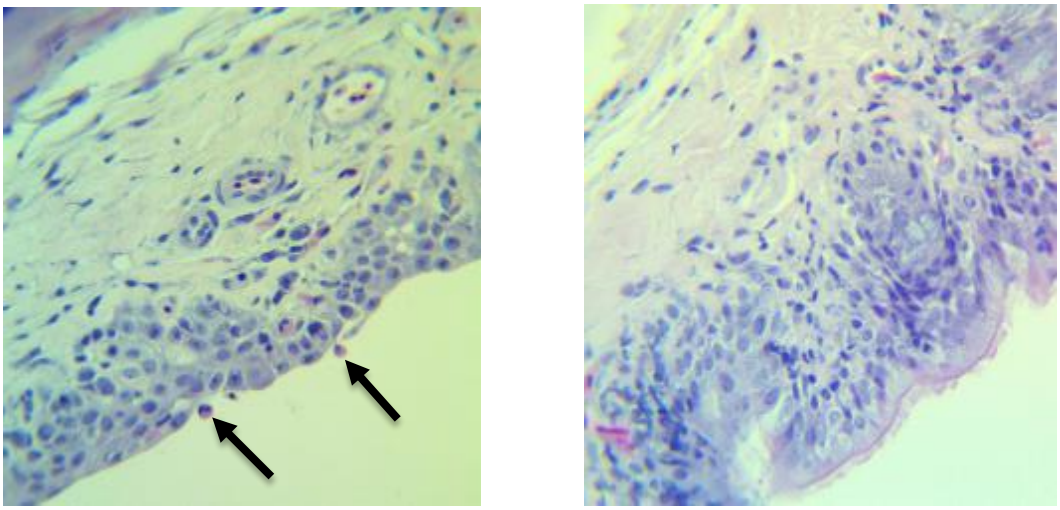

Figure 14. Mucosal lining of the trachea of an affected bird infiltrated by small numbers of lymphocytes and macrophages (left) and the trachea of a control bird (right).

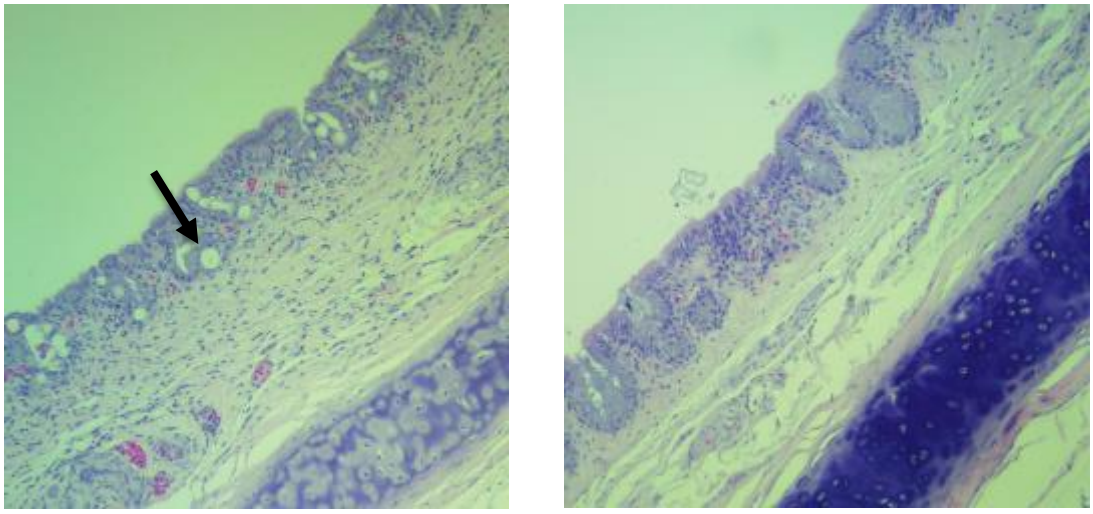

Figure 15. Vacuolated epithelial cells in the trachea of an affected bird (left) and the trachea of a negative control.

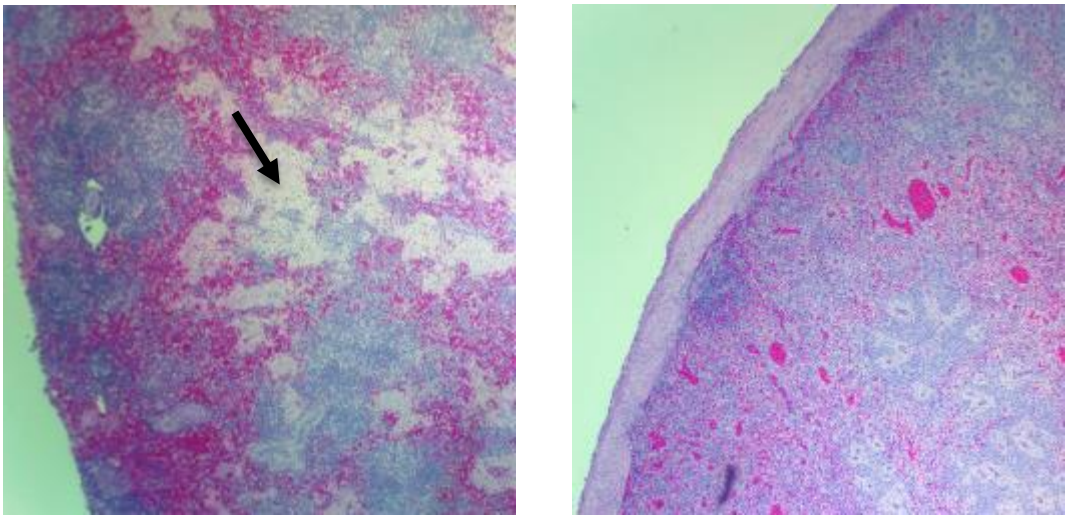

Figure 16. Lymphiod depletion in the spleen and multiple foci with the sinusoids containing fibrin (left) and control (right).

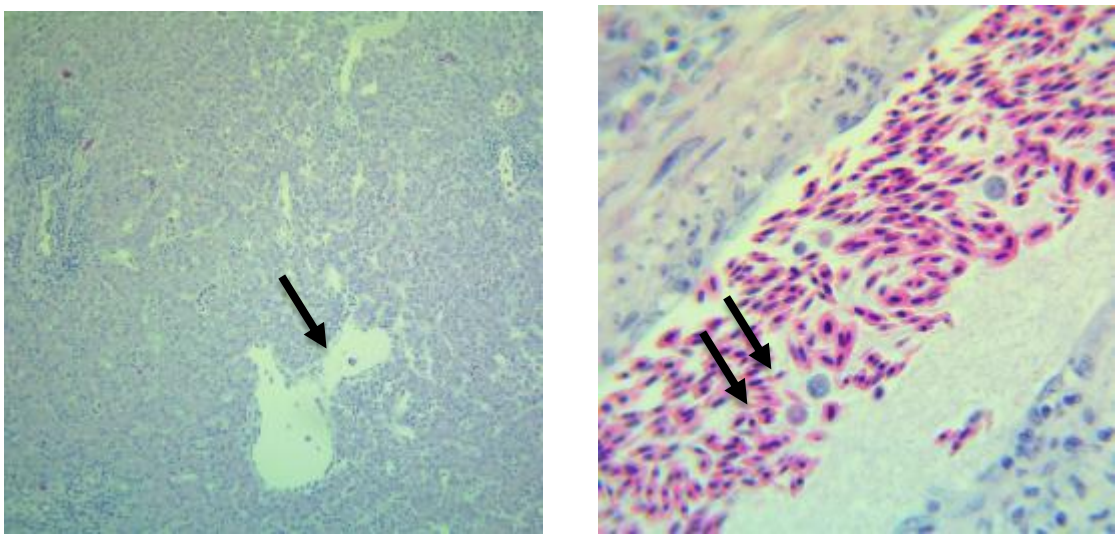

Figure 17. Acute necrosis of the liver, infiltrated by small numbers of heterophils, lymphocytes, and macrophages in the hepatic parenchyma (left). Portal tracts of the liver containing heterophils, lymphocytes, and macrophages (right).

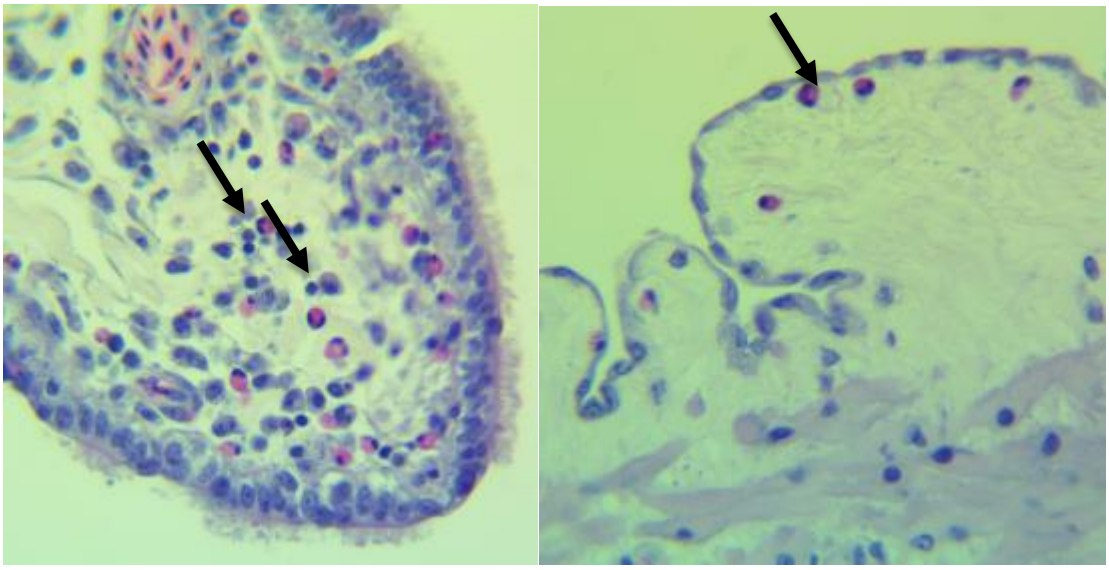

Figure 18. The oviduct inflitrated by small numbers of heterophils, lymphocytes, and macrophages.

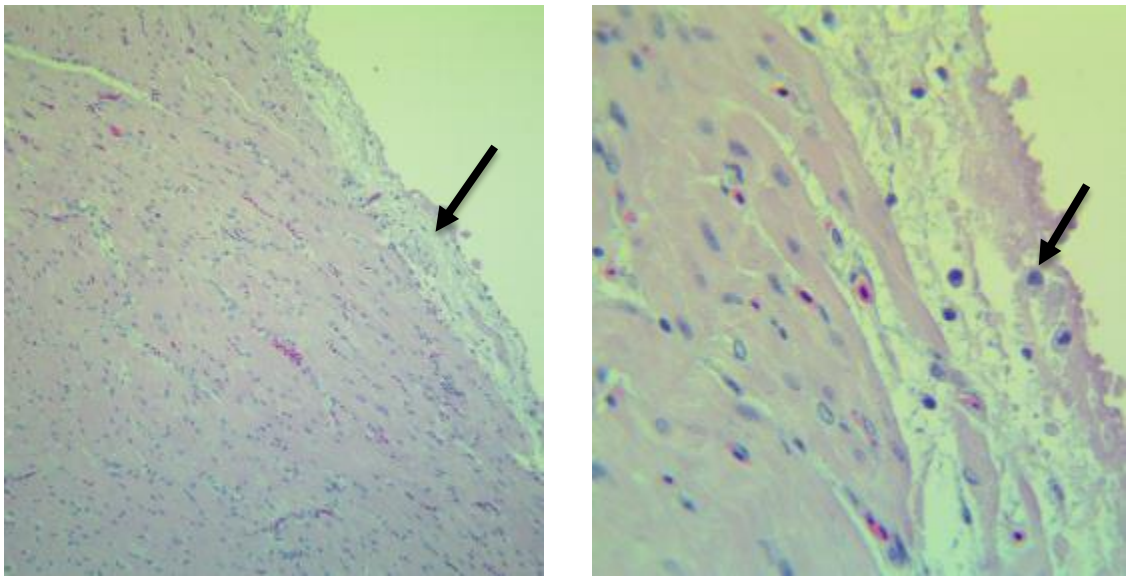

Figure 19. Fibrin and degenerated inflammatory cells covering the epicardium and a moderate number of macrophages, lymphocytes, and heterophils infiltrating the epicardium.

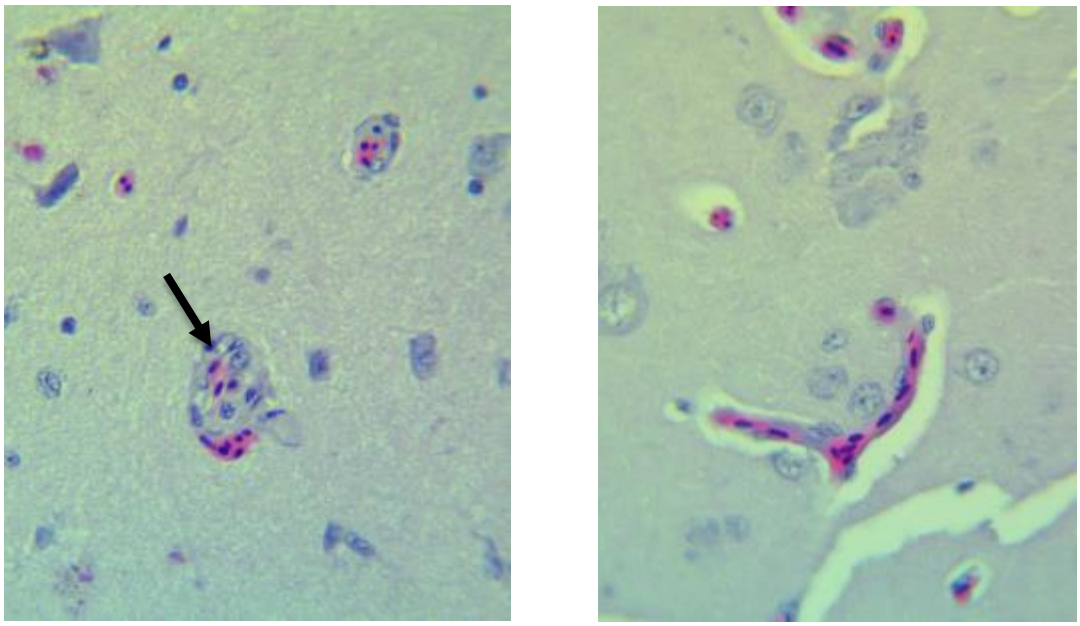

Figure 20. The medium-sized blood vessels of the brain cuffed by small numbers lymphocytes (left) and the brain of a control bird (right).

Conclusion

Despite the massive devastation it caused, very little is known about the specific virus, particularly regarding its distribution and lesions caused within the turkey host during the outbreak. It was unknown as to why there was a very small population of turkeys that would survive the massive mortality and appear unaffected several days later. We now know that all of the birds were indeed infected but the viral load and presence was very different in the clinically affected versus sub-clinically affected. The viral load was higher in the brain, GI, spleen, and trachea of the clinically affected birds. The increased viral concentration in the brain most likely contributed to the neurological symptoms observed in the clinically affected turkeys.

Histological changes and lesions were generally mild and insignificant. Changes were predominantly seen in the liver and the trachea and primarily consisted of the infiltration of small numbers of heterophils, lymphocytes, and macrophages. The liver had the lowest concentration of virus yet some of the most changes. The mechanisms and subsequent reasoning behind these observations need to be further explained. Based on the lack of pathological and histological lesions, some mechanism other than multi-organ necrosis was responsible for the fatal outcome.

This study is the first of its kind that provides virus distribution and semi-quantitate matrix gene analysis across multiple tissues in the turkey. It is also the first of its kind that characterizes the differences in distribution and matrix gene levels between

clinical and sub-clinical birds. The virus appeared to replicate more rapidly in the clinically affected birds, particularly in the brain and reproductive tracts. Understanding why the difference was seen is important in understanding the virus-host interaction. Due to the propensity and virulence of the virus and barn design, it can be assumed that all birds were exposed to the virus within a very short time frame. The reasons as to why a small portion of the birds survived the massive mortality on day 2 and were sub-clinical 4 days after the matrix gene was first detected in the barn has yet to be explained. Although the virus was found in all of the tissues, the exact location in the tissues needs to be elucidated.

CHAPTER III

GENE EXPRESSION

Overview

The outbreak of the highly pathogenic avian influenza virus (HPAI) in 2014-2015 was by far the largest animal disease outbreak in United States history. The turkey industry was the most affected with nearly 70% of the confirmed cases were in turkeys. Minimal research has been done on the effects of HPAI infection on turkeys, particularly on the subject of host response. This study examined changes in the gene expression of several components across 8 different tissues: brain, heart, GI, liver, lung, reproductive tract, spleen and trachea. The pro-inflammatory cytokines IL-1β and IL-6, the anti-inflammatory cytokine IL-10, and chemokines CCL-5 and CXCLi-2 were studied as well as the antiviral components Mx, OASL, and IFN-γ, IFIH1 the gene that encodes for the MDA5 signaling mechanism, and the death ligands FasL and TRAIL The results are indicative that the virus was very efficient at evading early detection and inhibiting anti-viral defenses.

There was no indication of an excessive pro-inflammatory response or pathogenesis induced by a cytokine storm. This particular virus was able to avoid initial detection by suppressing the expression of viral detecting mechanisms, pro-inflammatory cytokines, and antiviral components in the trachea. Undetected, the virus quickly disseminated throughout the body and replicated very rapidly. A widespread

downregulation of IFN-γ and upregulation mRNA expression of CCL-5 and OASL appeared to contribute to the pathogenesis. Death was a result of viral load in the tissues and subsequent organ failure.

Introduction

Avian influenza (AI) viruses are part of the Orthomyxoviridae family and genus Influenzavirus (Suarez, 2008). The entire viral genome consists of eight single-stranded, negative sense, RNA segments (Perdue, 2008; Adam and Sandrock, 2010). The surface is covered with two types of glycoprotein projections; hemagglutinin (HA) and neuraminidase (NA) (Vasin et al., 2014). While the HPAI virus and host interaction has been described to an extent in the chicken and duck (Blyth et al., 2016; Cardona et al., 2008; Kuchipudi et al., 2012; Swayne, 2008), published literature regarding HPAI infections in turkeys is scarce. It is also unlikely that what has been previously seen in with regards to immune response in the chicken is applicable to the turkey, as immune-mechanisms between the species is different (Arsenault et al., 2014). The HPAI H5N2 virus involved in the 2014-2015 outbreak was shown to have reduced adaptation and transmissibility in the chicken when compared to the turkey (data pending pub.). Nearly 70% of cases reported during the outbreak involved turkeys (USDA-APHIS, 2015). This would not be the first time that the turkey was known to respond differently to the same pathogen and lead to increased pathogenesis (Powell et al., 2009).

Even with a highly evolved and complex immune system in the host, AI viruses are still able to evade it. Virulence can be correlated with immune evasion (Perdue, 2008; Swayne and Suarez, 2000). Avian influenza viruses use several tactics to elude the immune system. The virus is known for its high mutability and reassortment capabilities (Perdue, 2008; Swayne and Suarez, 2000). Mutating or reassorting changes the specificity of the antibody needed for host protection, thus resulting in increased viral replication and transmission of mutated strains (Hale et al., 2010. The non-structural (NS) viral proteins are critical in immune evasion. The NS1 protein can limit the production and effectiveness of the interferons, which inhibit viral replication, (Hale et al., 2010) by blocking the cytoplasmic RIG-I/MDA5 signaling cascade or by attenuating INF-inducible signaling (Hale et al., 2010 and Vijayakumar et al., 2015). The protein can suppress the Fas/Fas-ligand-mediated apoptosis thus increasing the infectivity (Xing et al., 2009). The virus can induce and/or inhibit cellular apoptosis of various cell types including immune cells (Ekchariyawat et al., 2011), increase viral replication speed (Hale et al., 2010) and induce cytokine deregulation of the host (Kuribayashi et al., 2013).

H5N2 Outbreak of 2014-2015

The outbreak of the Highly Pathogenic Avian Influenza Virus (HPAI) in 2014-2015 was by far the largest animal disease outbreak in United States history. Within six months of its first detection, HPAI H5N2 destroyed nearly 50 million birds in 21 states, making it the largest animal disease outbreak in United States history (UDSA-APHIS,

2015). It devastated the egg laying and turkey industries in the upper Midwest and cost the government over $950 million to stop the disease.

The present study provides insight to understanding the host response in naturally infected turkeys. This study examined changes in the transcription of several host defense genes across 8 different tissues: brain, heart, GI, liver, lung, reproductive tract, spleen and trachea. The pro-inflammatory cytokines IL-1β and IL-6, the anti-inflammatory cytokine IL-10, and chemokines CCL-5 and CXCLi-2 were studied as well as the antiviral components Mx, OASL, and IFN-γ, IFIH1 the gene that encodes for the MDA5 signaling mechanism, and the death ligands FasL and TRAIL. This is the first study of its kind that characterizes the 2014-2015 HPAI H5N2 virus in naturally infected turkey breeder hens with regards to the host response. This information enhances the general understanding and properties of the virus and host interaction during the turkey during the spring 2015 outbreak of HPAI H5N2.

Materials and Methods

RNA Extraction

RNA extraction was completed at the University of Minnesota's Mid-Central Research and Outreach Center in Willmar, MN. Four birds from each of the groups, a total of 12 birds per tissue, were selected for RNA extraction. The RNA was extracted from the tissues using an RNeasy® Mini Kit (Qiagen) and prefilled 2 mL tubes

containing MagNA® Lyser Green Beads (Roche Life Science®, Indianapolis, IN). Prior to starting, 600 µL of Buffer RLT and β-mercaptoethanol (β-ME) (Qiagen), mixed at a rate of 1 µL β-ME to 1 mL Buffer RLT, was added to each MagNA® Lyser tubes. Approximately 30 mg of tissue was placed in the MagNA® Lyser Green Bead tubes and homogenized using a MagNA® Lyser instrument at 8000 x g for 90 seconds. MagNA® Lyser Green Bead tubes were then centrifuged at 8000 × g. Next, 350 µL of the supernatant was pipetted into a new 2 mL microcentrifuge tube along with 350 µL of 70% ethanol and thoroughly mixed via a pipette. The solution was transferred to an RNeasy® spin column and centrifuged at 8000 × g speed for 30 seconds. The flow-through was discarded. Then, 700 µL of RW1 Buffer (Qiagen) was added to the column and the column was spun at 8000 × g for 30 seconds. The flow through was again discarded. Next, 500 µL of RPE Buffer (Qiagen) was added to the column and spun for 30 seconds at 8000 × g. The flow-through was discarded and an additional 500 µL of RPE Buffer was added to the column and spun for 2 minutes. The column was then transferred into a new 2 mL collection tube and spun at maximum speed for 1 minute. The column was then transferred into a 1.5 mL collection tube and 50 µL of RNase free water (Qiagen) was added. The column was spun at 8000 × x g for 1 minute and the RNA elute was aliquoted into 4, 10 µL samples, and stored at -80 °C.

Reverse Transcription

Reverse transcription and subsequent gene analysis took place in Dr. Zheng Xing's lab at the University of Minnesota-St. Paul campus. The quality and quantity of

the RNA was assessed using a NanoDrop® spectrophotometer. The RNA was reverse transcribed to complementary deoxyribonucleic acid (c-DNA) using a QuantiTect® Reverse Transcription Kit (Qiagen). Genomic DNA elimination reactions were carried out using 2 µL of gDNA Wipeout Buffer 7× and a combination of template RNA and RNase-free water of various quantities to equal 500 ng/µL for a total of 12 µL. Solution was then incubated at 42 ºC for two minutes and held on ice. Reverse transcription reactions were carried out by mixing the previously incubated solution with 6 µL of reverse-transcription master mix. Master mix was comprised of 1 µL of Quantiscript® Reverse Transcriptase, 4 µL of Quantiscript® RT Buffer 5×, and 1 µL of RT Primer Mix per each reaction. Solutions were then incubated for 15 minutes at 42 ºC to initiate reverse transcription and then 3 minutes at 95 ºC to inactivate the Quantiscript® Reverse Transcriptase.

Real-Time qPCR

A total of 8 birds were run per tissue, 3 clinical, 3 non-clinical, and 2 negative controls. Each of the eight tissues were run on separate 96 well plates. The endogenous housekeeping gene, GAPDH was used as a standard control for changes in gene expression. Cytokines IL-1β, IL-6, CXCLi-2, IL-10, CCL-5, IFN-γ, Mx, OASL, IFIH1, FasL and TRAIL were ultimately examined. Based on previously published data and with the help of Primer 3 software, Dr. Xing designed and acquired the primers. See Table 1 below for primer sequences. Primers were diluted with RNase-free water to 10 µM. Each PCR reaction was set up as follows: 0.5 µL of specific cytokine 5’ primer, 0.5

µL of the specific cytokine 3’ primer, 0.7 µL of reverse transcribed mRNA, 4.75 µL of dH_2O, and 6.25 µL of 2× SYBR® Green PCR Master Mix (Applied Biosystems®, Carlsbad, CA).

Gene	Forward 5’ Primer	Reverse 3’ Primer
GAPDH	gacgtgcagcaggaacacta	cttggactttgccagagagg
IL-1β	ctctacatgtcgtgcgtgct	ctgtccaggcggtagaagac
IL-6	gacgaggagaaatgcctgag	agcgattcgacattctgctt
CXCLi-2	ccactgcaagaacgttgaaa	ggccataagtgcctttacga
IL-10	aagcgctgtcaccacttctt	tcccgttctcatccatcttc
CCL-5	cgcctacatcactagcagca	agttccaggtggttctgcac
IFN-γ	agccgcacatcaaacacata	catctgaagctttgccaggt
Mx	atgtgctgcaacaagcaaag	tcctgcaaggaaaagcatct
OASL	caccacaagctggagcacta	atagctcaggagggcacaaa
IFIH1	aaaggcccaagaaaggaaaa	ttccatgaatgcacaccact
FasL	gtggtgctgttgaaatgtgg	ggttttggcaacacaggact
TRAIL	gaggactcggatttgttgga	atgagcagaatgggatctgg

Table 4. Primer sequences

The plates were then run on an Applied Biosystems® 7500 Real-Time PCR System with standard cycling conditions. See Table 4 for cycling conditions. Melting curves and amplification plots were analyzed for specificity. Results were expressed as Ct values and standardized to the changes seen with GAPDH and the two separate internal controls. Fold changes were calculated using the universally accepted $2^{-\Delta\Delta}$Ct for each of the tissues and cytokines. Statistical analysis of the fold and gene expression changes of the ΔCt was carried out using a Student's T-test using the JMP® Pro 12 software for Windows (Microsoft, USA). Probability (p)-values <0.05 were considered statistically significant.

Stage	**Reps**	**Temp**	**Time**
1	1	50ºC	1 min
2	1	95ºC	5 min
3	40	95ºC 58ºC	15 sec 32 sec
4	1	95ºC 60ºC 95ºC	15 sec 1 min 15 sec

Table 5. PCR cycling conditions used in gene expression analysis.

Gene Expression

The primer sequences designed for IFN-α and IFN-β did not work, therefore IFN-γ was used. It is not known if the sequence wasn't designed correctly or if there were other reasons unique to the turkey, as the turkey genome is poorly annotated. While IFN-α and IFN-β have been studied in the chicken, IFN-γ is the only IFN documented in the turkey thus far (Gadde et al., 2011, Mondal et al., 2013 and Umar et al., 2016). Gene expression was analyzed using two different group configurations. In the first configuration, all the positive birds were grouped together, regardless of clinical status, and compared to the negative controls. In the second configuration, the positives were sub-divided into clinical and sub-clinical groups and compared against each other as well as the negative control birds. Some tissues and cytokines were more difficult to obtain results from than others. The brain and reproductive tract were the most difficult tissues. In the previous study, these tissues had also had the highest concentration of viral load. It is unknown it contributed to the problems. Of the genes, IL-10 was the most problematic. Issues with IL-10 may possibly be tissue related. Similar to the current study, we previously were able to successfully study IL-10 across multiple areas of the GI tract without problem. When IL-10 was initially characterized in the turkey, expression in the GI was found to be consistent however expression in non-lymphoid tissues was found to be highly variable (Powell et al., 2012). Variation in cytokine response among individuals in a given population was seen with the current study but has been previously reported (Adams, 2009). Despite the obstacles, significant changes were seen with multiple cytokines in a number of tissues throughout the body.

Brain

It is uncertain as to why, but the brain was by far the most difficult of the eight tissues collected to obtain gene expression results. Gene expression in the turkey brain has not yet been studied. As a result of the gene expression challenges, some of the data are incomplete. Obtaining changes in the expression of IL-10, FasL, and IFIH1 for any of the groups and IL-1β, IL-6, and CXCLi-2 for the sub-clinical group was unsuccessful. Regardless of the gaps in the data, meaningful data were acquired. The changes seen with regards to anti-inflammatory cytokine expression in the brain were minimal compared to the anti-viral gene expression. Changes in IL-1β were negligible in the brains of the clinically affected birds, but IL-6 was significantly upregulated, 18.81 fold. Anti-inflammatory data were not obtained in the brain. The chemokine CCL-5 was significantly upregulated in the brains of clinically, 16.65 fold, and sub-clinically affected birds, 10.06 fold as well as in the positive group, 13.36 fold. Expression in the clinical and sub-clinical birds were statistically different from the negative controls as well as from each other. The antiviral gene Mx was significantly upregulated in the positive group, 3.15 fold, compared to the negative group. The clinically affected birds had significant upregulation of OASL, 256.58 fold, in the brain. IFN-γ was significantly down regulated, -1.52 fold, in the clinically affected, when compared to the sub-clinical and negative controls. The sub-clinical birds had a slight upregulation, 1.48 fold, of IFN-γ. See figures 1-3.

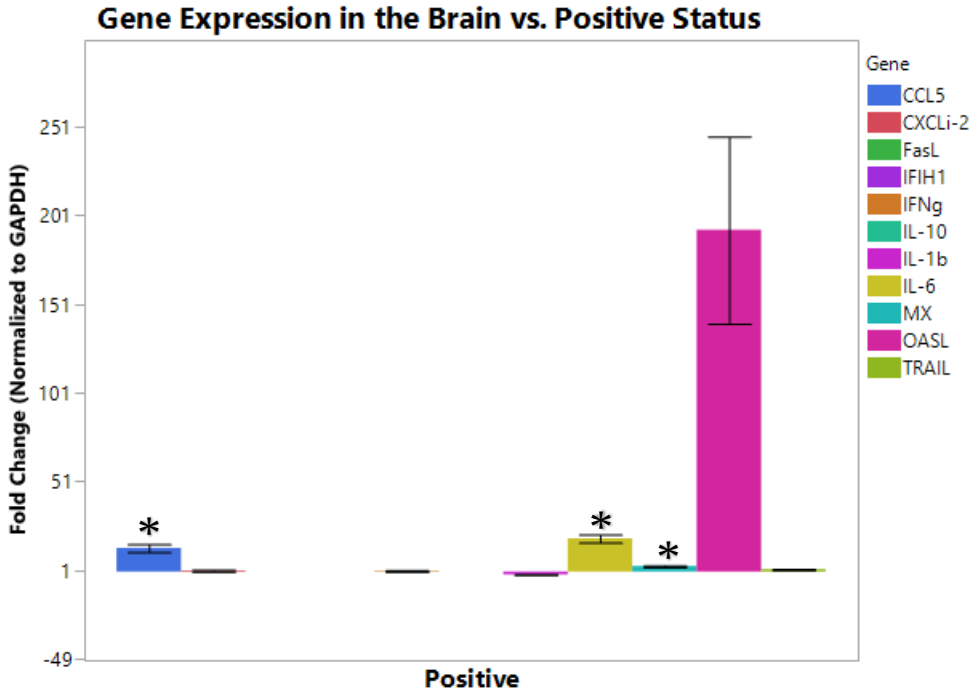

Figure 21. Gene expression in the brain of positive birds. "*" denotes significant difference from controls. P-values <0.05 were considered to be significant.

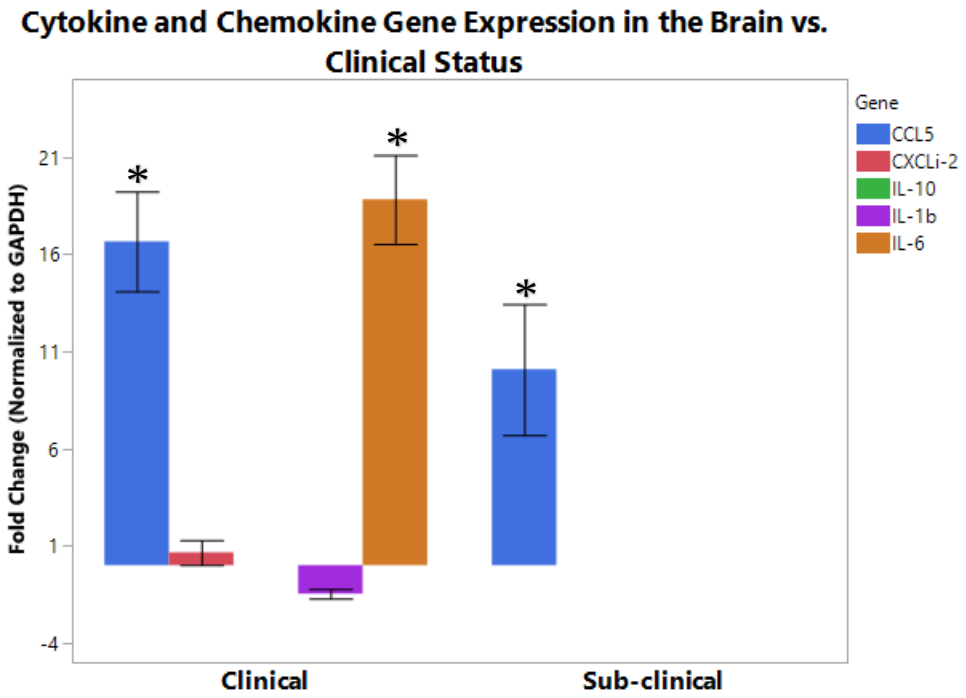

Figure 22. Cytokine and chemokine gene expression in the brain *vs.* clinical status. "*" denotes significant difference from controls. P-values <0.05 were considered to be significant.

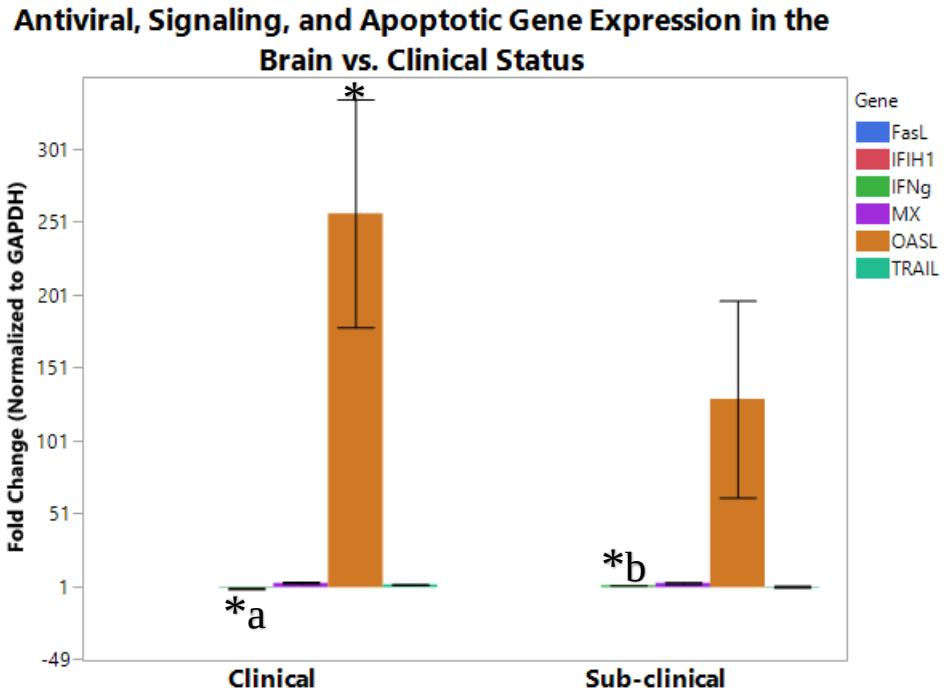

Figure 23. Antiviral, signaling, and apoptotic gene expression in the brain *vs.* clinical status. "*" denotes significant difference from controls. "a/b" denotes significant difference between clinical and sub-clinical groups. P-values <0.05 were considered to be significant.

GI

Several differences were noted in gene expression in the GI. CCl-5 and OASL were significantly upregulated in the positive group, 4.58 and 25.77 fold respectively. Whereas, IFN-γ was significantly downregulated nearly 2 fold in the positive group. Changes in neither of the pro-inflammatory cytokines or anti-inflammatory cytokine were significant in the GI. Both chemokines, CCL-5 and CXCLi-2 were upregulated. In the clinically affected cases, CCL-5 was significantly upregulated from the controls,

4.88 fold. As was Mx and OASL, 14.51 and 30.0 fold respectively. IFN-γ was significantly down regulated -1.25 fold. See figures 4-6.

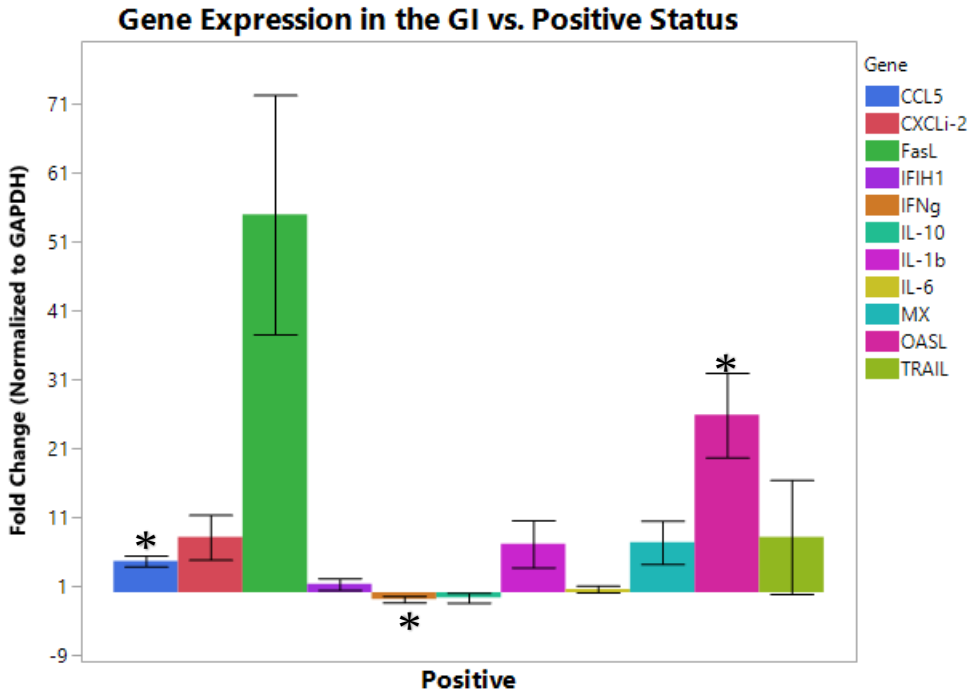

Figure 24. Gene expression in the GI of positive birds. "*" denotes significant difference from controls. P-values <0.05 were considered to be significant.

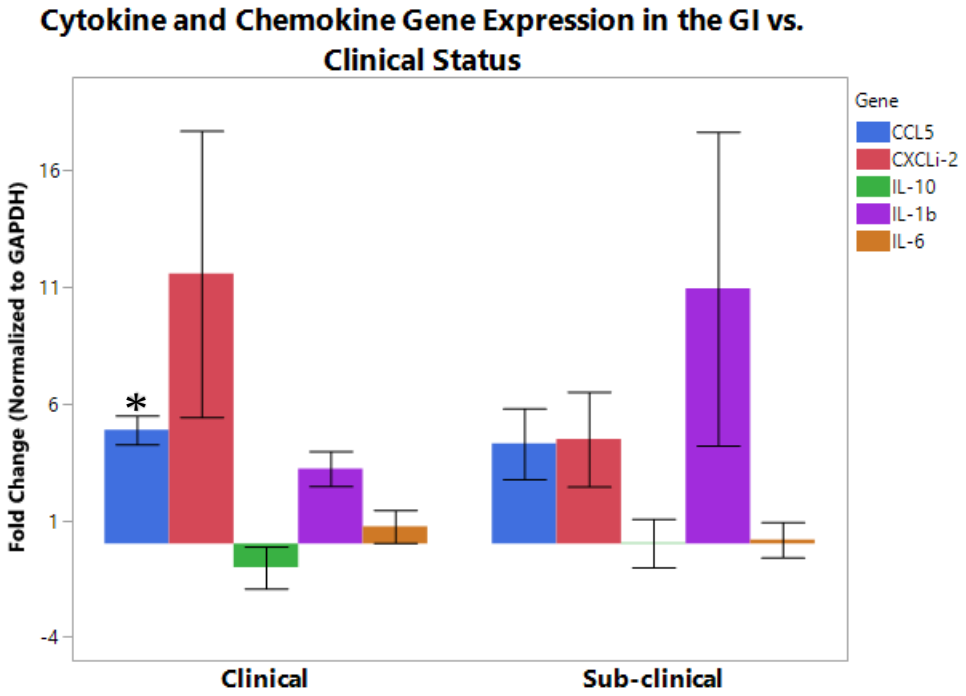

Figure 25. Cytokine and chemokine gene expression in the GI *vs.* clinical status. "*" denotes significant difference from controls. P-values <0.05 were considered to be significant.

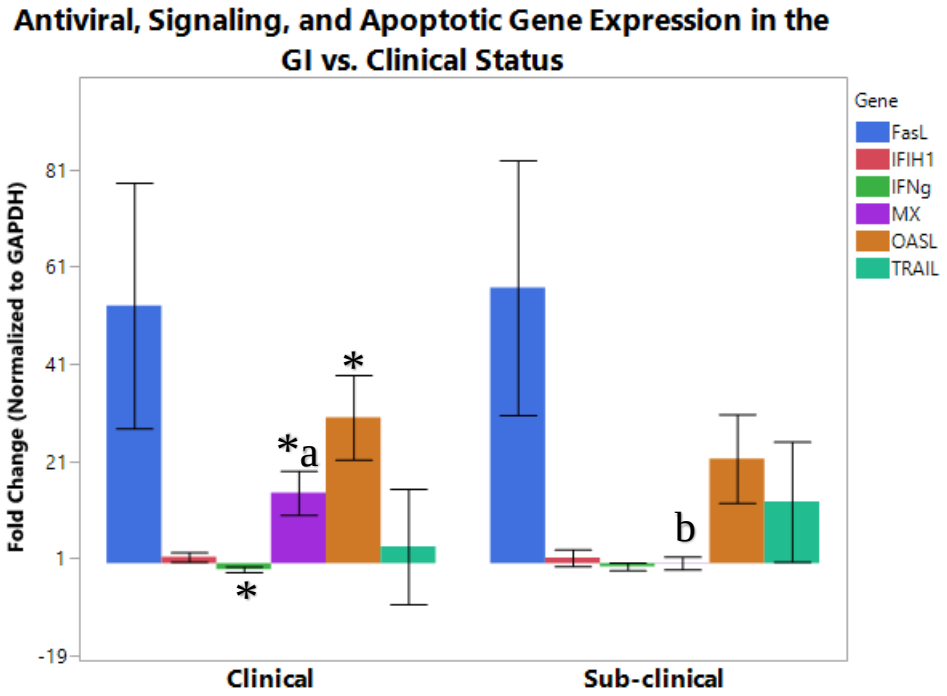

Figure 26. Antiviral, signaling, and apoptotic gene expression in the GI *vs.* clinical status. "*" denotes significant difference from controls. "a/b" denotes significant difference between clinical and sub-clinical groups. P-values <0.05 were considered to be significant.

Heart

No IL-10 data were obtained for the heart. Both pro-inflammatory cytokines were significantly upregulated in the positive birds. IL-1β was upregulated 3.23 fold and IL-6 was upregulated 12.81 fold. IFIH1 was also significantly upregulated in that group by 8.49 fold. Clinically affected birds had a significant upregulation of IL-1β, 8.84 fold, CCL-5, 81.76 fold, OASL, 459.93 fold, and IFIH1, 8.84 fold. The sub-clinical birds had an upregulation of IL-6, 12.43 fold. They were also considered statistically different than

the clinical birds regarding CCL-5 at 20.84 fold and OASL at 91.64 fold. See figures 7-9.

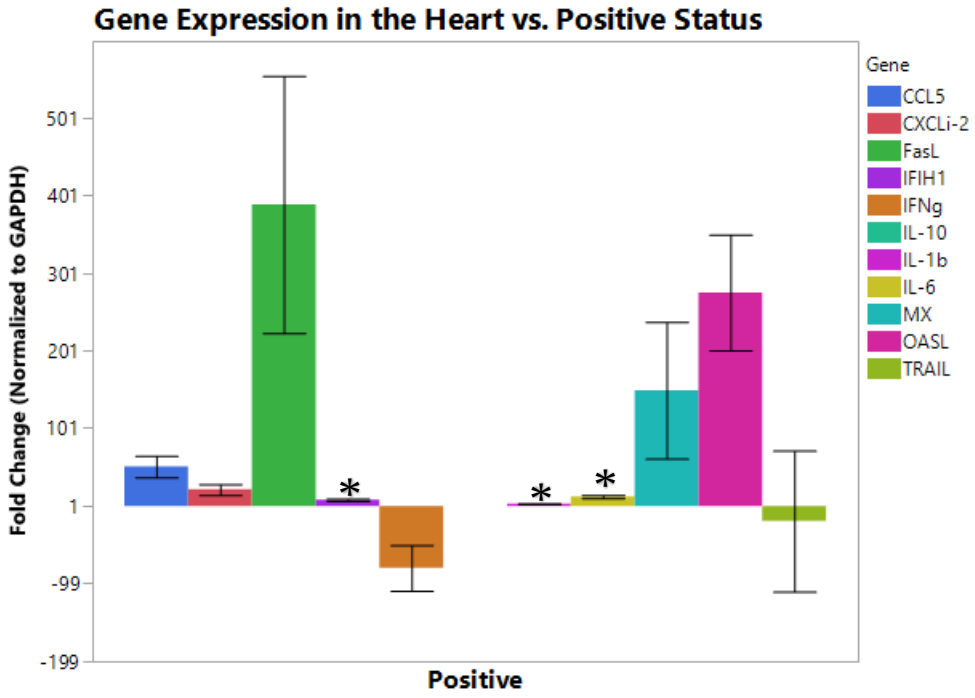

Figure 27. Gene expression in the heart of positive birds. "*" denotes significant difference from controls. P-values <0.05 were considered to be significant.

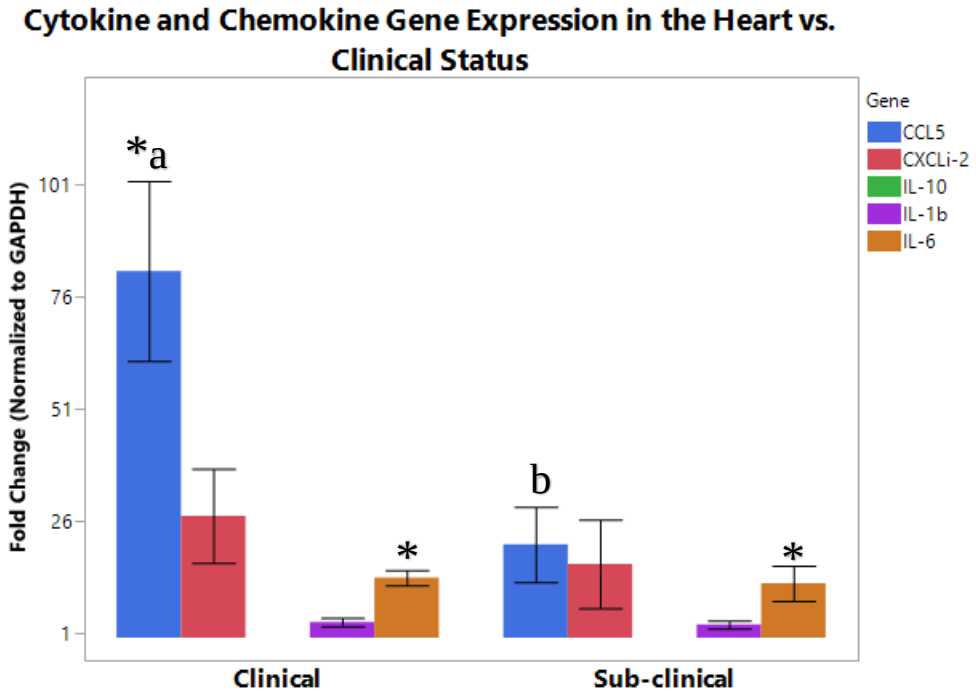

Figure 28. Cytokine and chemokine gene expression in the heart *vs.* clinical status. "*" denotes significant difference from controls. "a/b" denotes significant difference between clinical and sub-clinical groups. P-values <0.05 were considered to be significant.

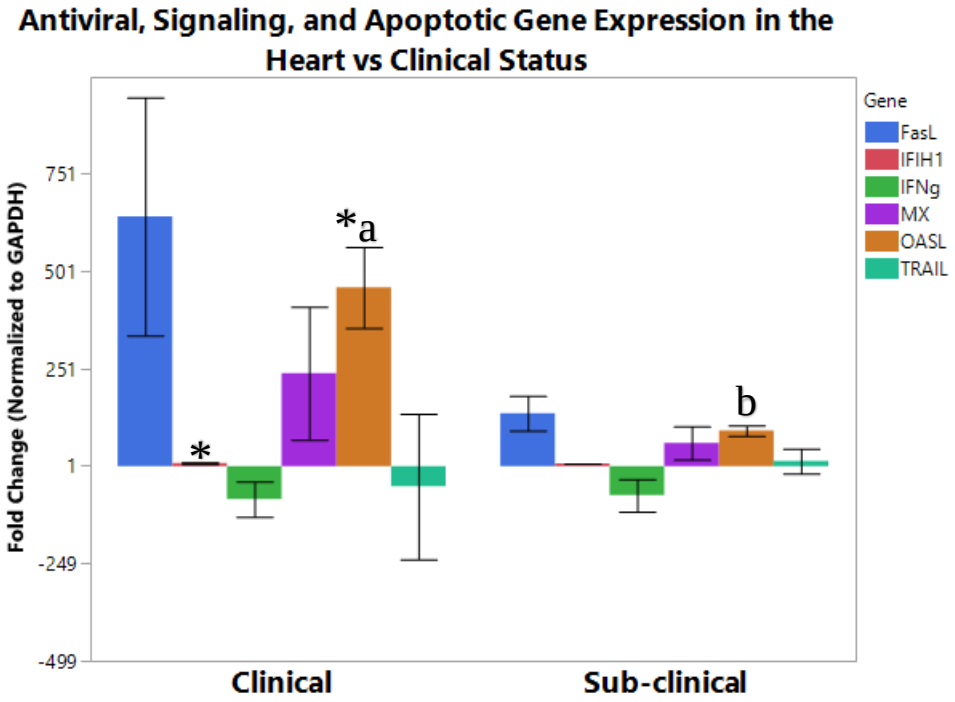

Figure 29. Antiviral, signaling, and apoptotic gene expression in the heart *vs.* clinical status. "*" denotes significant difference from controls. "a/b" denotes significant difference between clinical and sub-clinical groups. P-values <0.05 were considered to be significant.

Liver

The positive birds had significantly higher expression of IFIH1, 1.42 fold, and OASL, 66.21 fold, and a downregulation of IFN-γ, -1.63 fold, in the liver. The clinically affected birds had higher IL-6, CCL-5, OASL, and IFIH1 expression, 2.1, 11.54, 72.19, and 1.54 fold respectively. They also had a down regulation in IFN-γ, -1.89 fold. FasL and OASL were up regulated in the sub-clinical birds, 64.23 and 60.23 fold. Meanwhile. IFN-γ and IL-6 were downregulated. See figures 10-12.

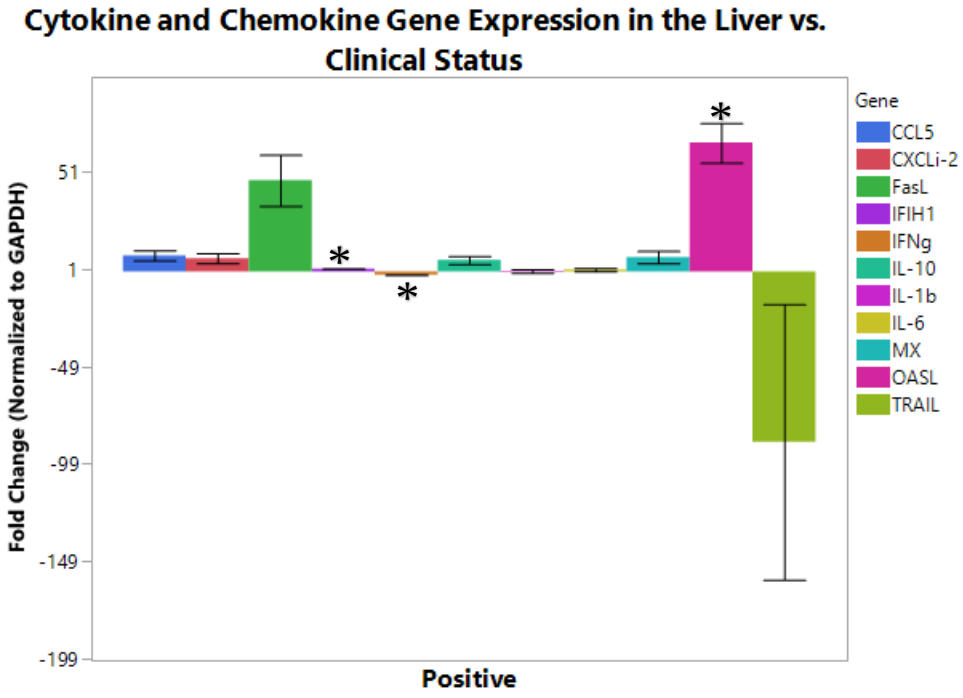

Figure 30. Gene expression in the liver of positive birds. "*" denotes significant difference from controls. P-values <0.05 were considered to be significant.

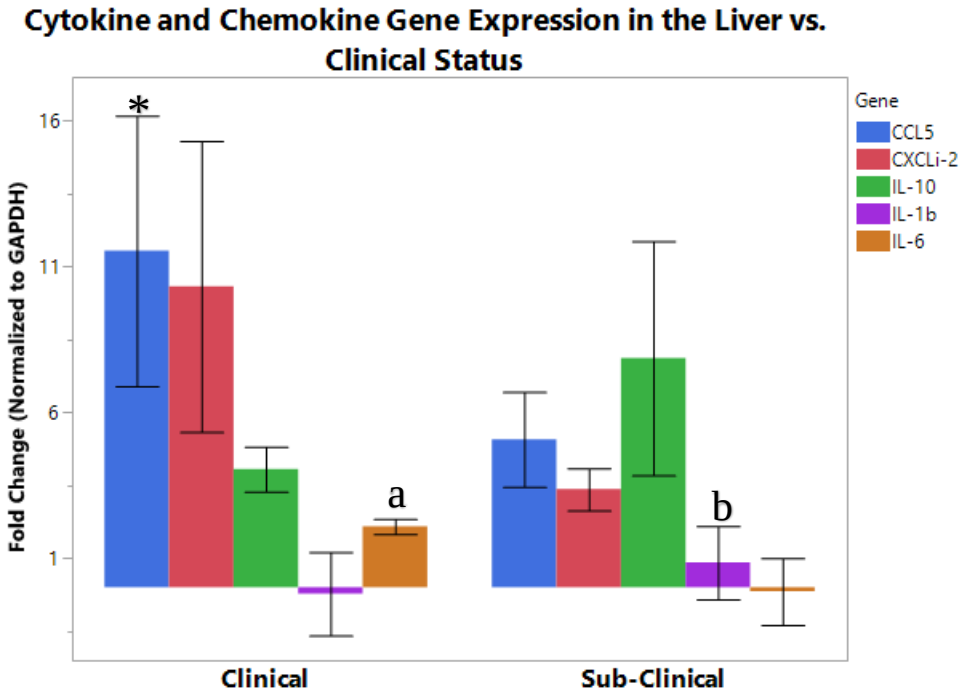

Figure 31. Cytokine and chemokine gene expression in the liver *vs.* clinical status. "*" denotes significant difference from controls. "a/b" denotes significant difference between clinical and sub-clinical groups. P-values <0.05 were considered to be significant.

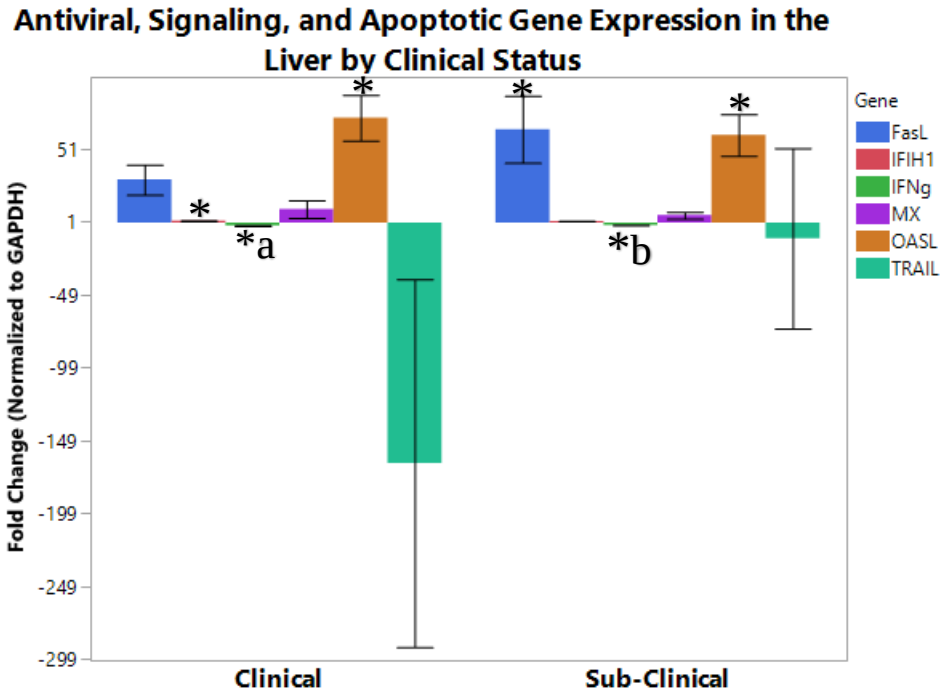

Figure 32. Antiviral, signaling, and apoptotic gene expression in the liver *vs.* clinical status. "*" denotes significant difference from controls. "a/b" denotes significant difference between clinical and sub-clinical groups. P-values <0.05 were considered to be significant.

Lung

The only significant changes in the lungs of the positive group of birds were with regards to IFN-γ. Its expression was significantly downregulated, 5.86 fold. Several significant differences were seen when looking at the clinical and sub-clinical groups. IL-1β was significantly different between the two groups, 2.17 fold in the clinical and 6.95 fold in the sub-clinical. The sub-clinical group was considered different than the

negative controls. In addition, both CCL5 and CXCLi-2 were expressed at a much higher rate than the controls, 13.74 fold and 6.66 fold respectively. The antiviral IFN-γ gene was downregulated, -9.89 fold, in the clinically affected and considered to be different than the controls as well as the sub-clinical group whose mean fold change was -3.16. OASL was significantly upregulated in the sub-clinical but not the clinical. See figures 13-15.

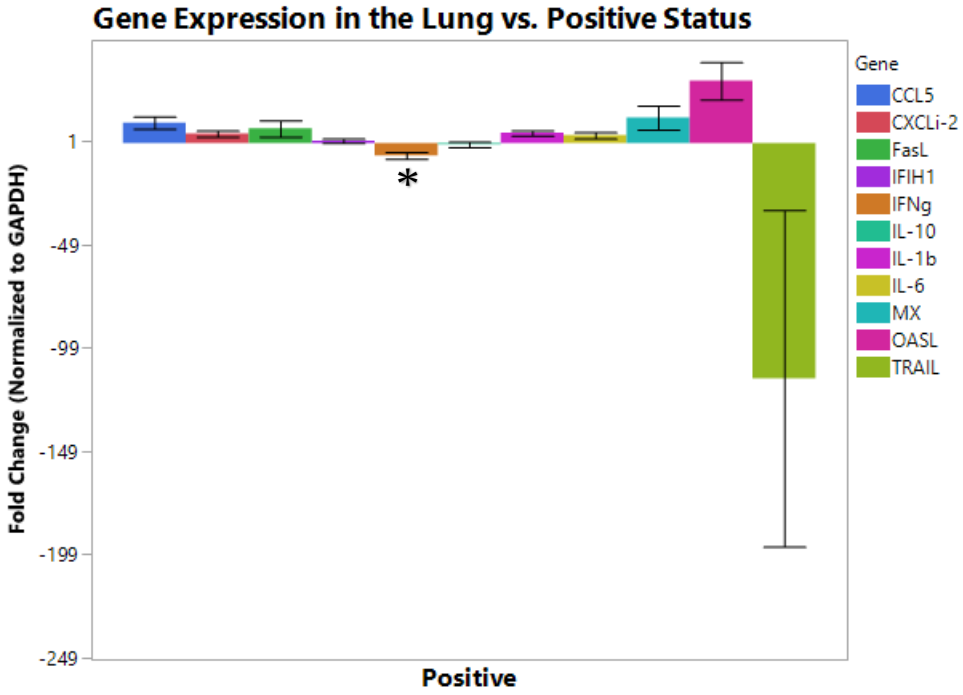

Figure 33. Gene expression in the lung of positive birds. "*" denotes significant difference from controls. P-values <0.05 were considered to be significant.

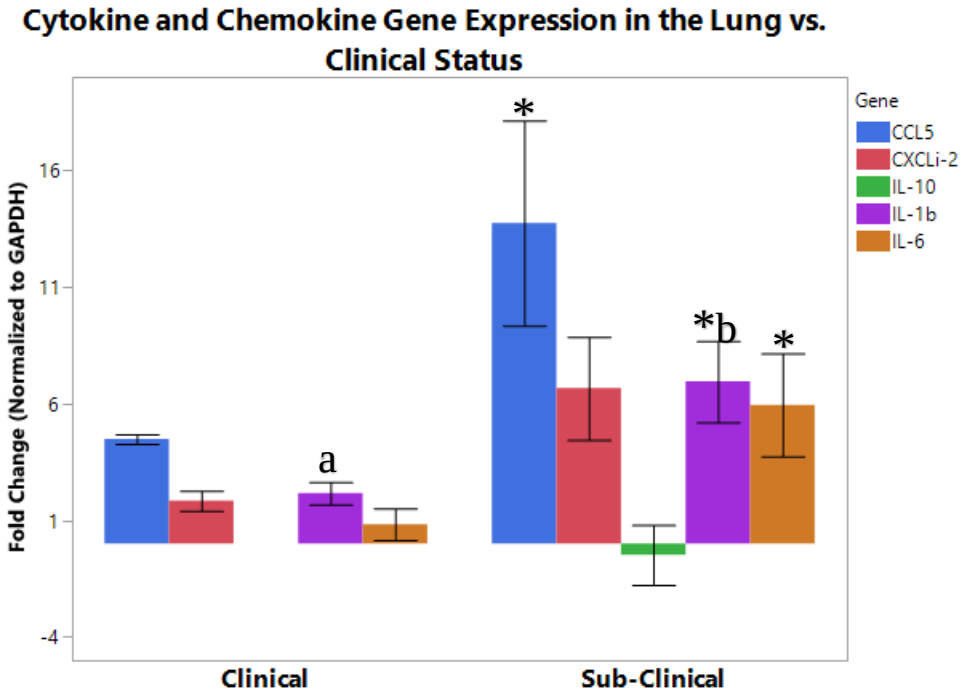

Figure 34. Cytokine and chemokine gene expression in the lung *vs.* clinical status. "*" denotes significant difference from controls. "a/b" denotes significant difference between clinical and sub-clinical groups. P-values <0.05 were considered to be significant.

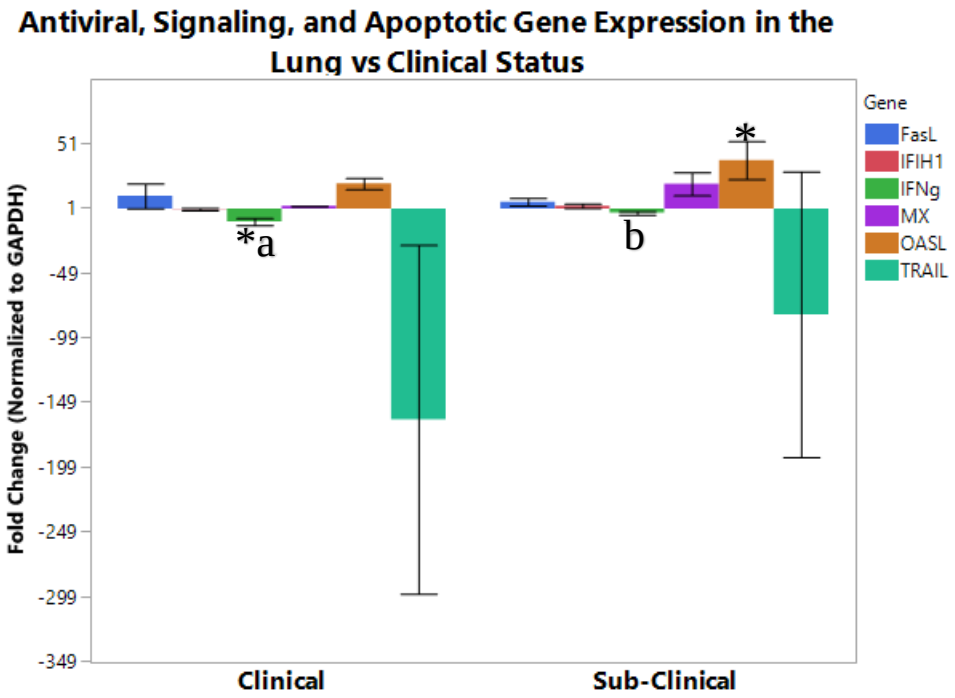

Figure 35. Antiviral, signaling, and apoptotic gene expression in the lung *vs.* clinical status. "*" denotes significant difference from controls. "a/b" denotes significant difference between clinical and sub-clinical groups. P-values <0.05 were considered to be significant.

Reproductive Tract

No IL-10 data was acquired for the reproductive tract. Although cytokine trends were seen with regard to the oviduct, cytokine variability and control bird issues resulted in statistically insignificant results. IL-1β, IL-6, CCL5, CXCLi-2, MX, OASL, and FAS tended to be upregulated while IFN-γ and TRAIL tended to be downregulated. See figures 16-18.

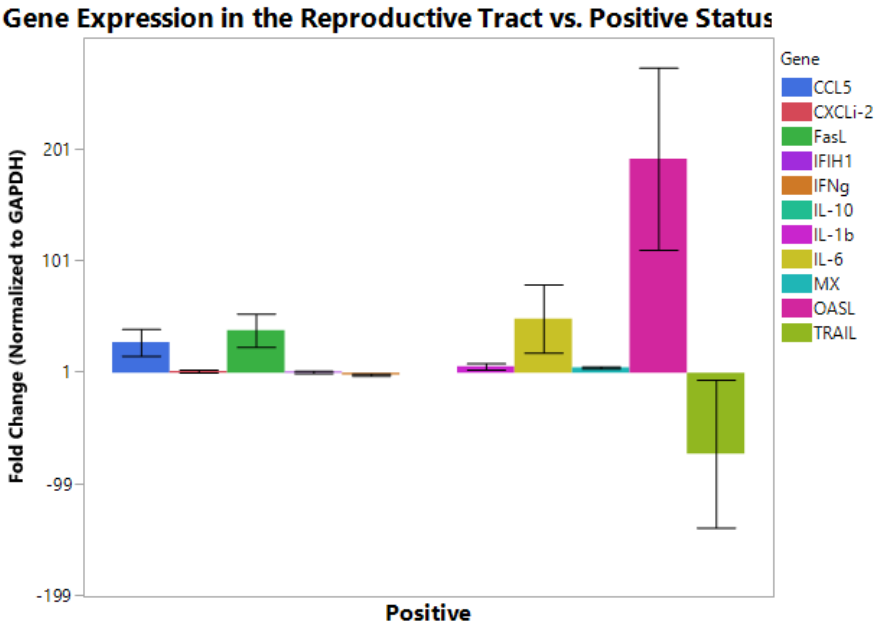

Figure 36. Gene expression in the oviduct of positive birds.

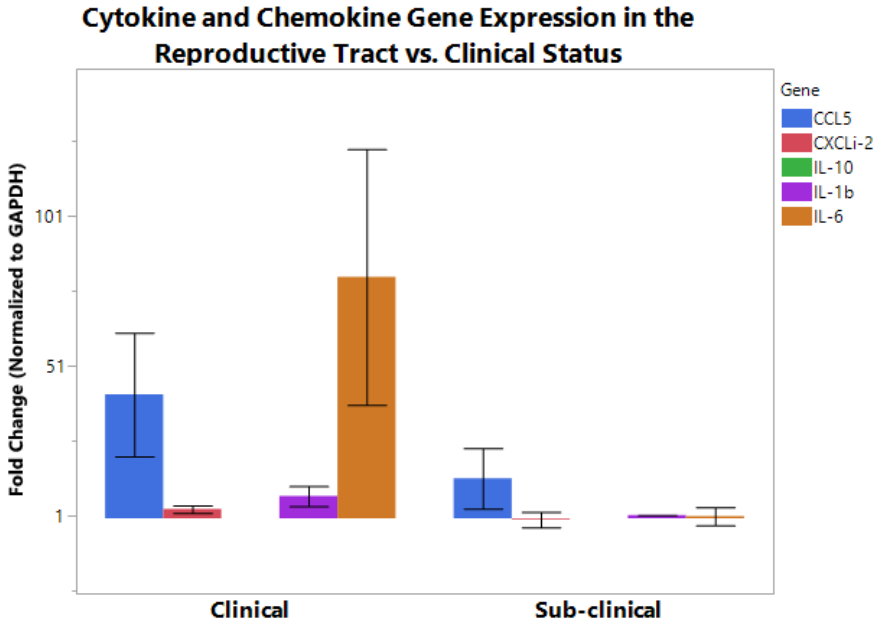

Figure 37. Cytokine and chemokine gene expression in the oviduct *vs.* clinical status.

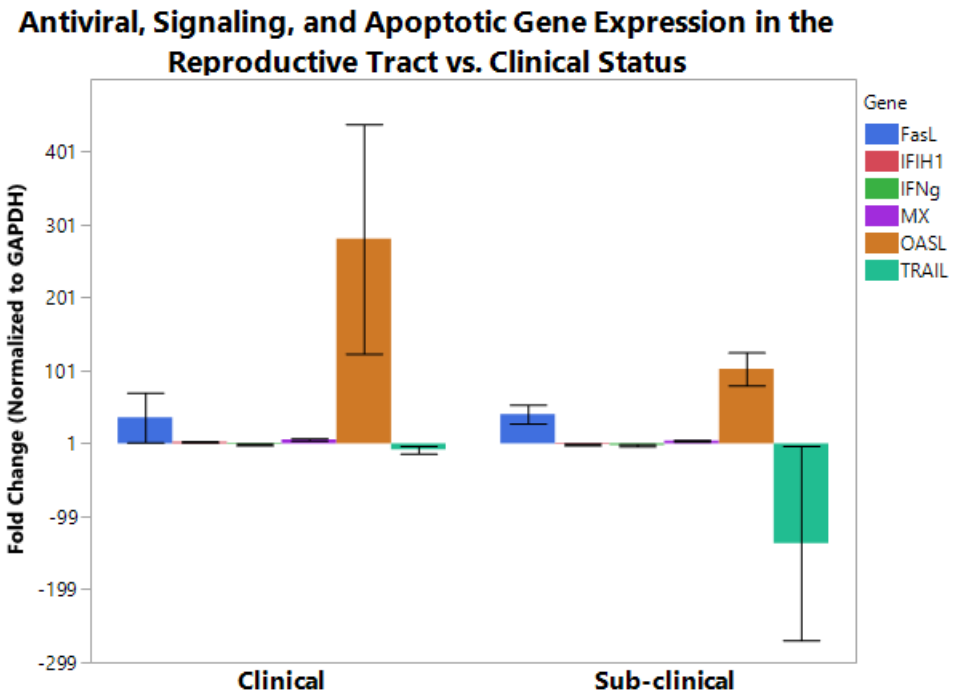

Figure 38. Antiviral, signaling, and apoptoic expression in the oviduct *vs.* clinical status.

Spleen

The spleen was very active with regards to cytokine activity. IL-1β and IFN-γ were significantly downregulated in the positive birds, -3.52 and -4.52 fold. On the contrary, expression of CCL5 and OASL were increased, 7.15 and 64.84 fold. Both the clinical and sub-clinical groups had significantly decreased levels of IL-β, -3.16 and -3.44 fold when compared to the control group. IL-6 in the clinical group was considered to be different than the expression seen in the sub-clinical group, 0.67 and -14.95 fold. CCL5 was significantly upregulated from the controls in the clinically affected and considered statistically different than the sub-clinically affected, 9.49 and 4.81 fold.

Expression of IFN-γ was decreased in both the clinical and sub-clinical groups, -5.24 and -3.8 fold. Mx was slightly upregulated in the clinically affected, 6.43 fold, and considered to be different than the sub-clinical that were slightly downregulated, -6.52 fold. OASL was significantly upregulated in the clinically affected group. Unlike the sub-clinical group which showed an increase in FasL, 5.58 fold, the clinically affected group showed a decrease in FasL, -3.06 fold. See figures 19-21.

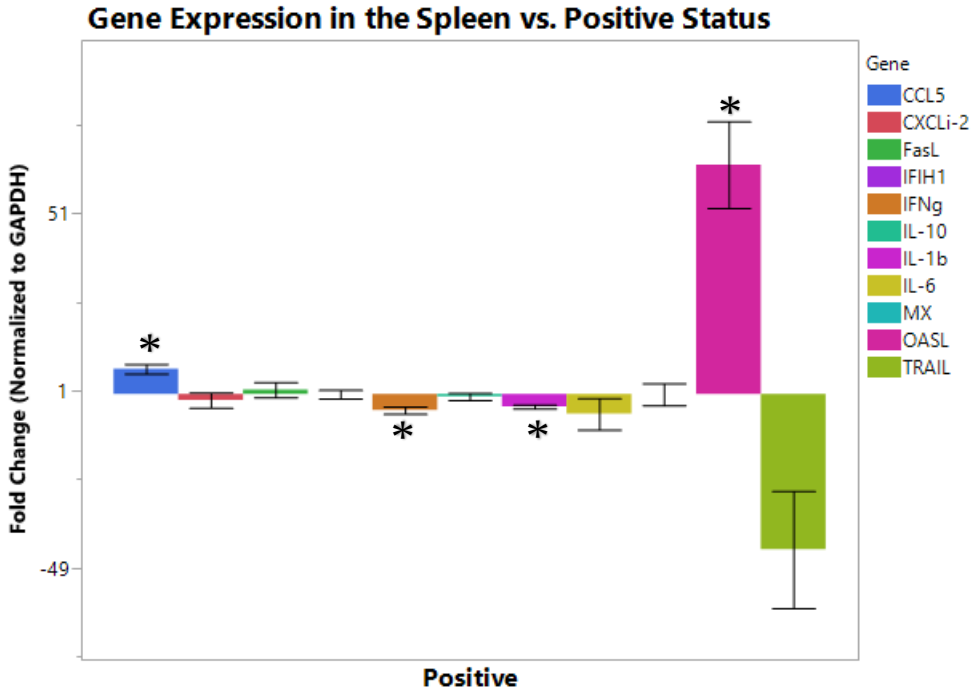

Figure 39. Gene expression in the spleen of positive birds. "*" denotes significant differencec from controls. P-values <0.05 were considered to be significant.

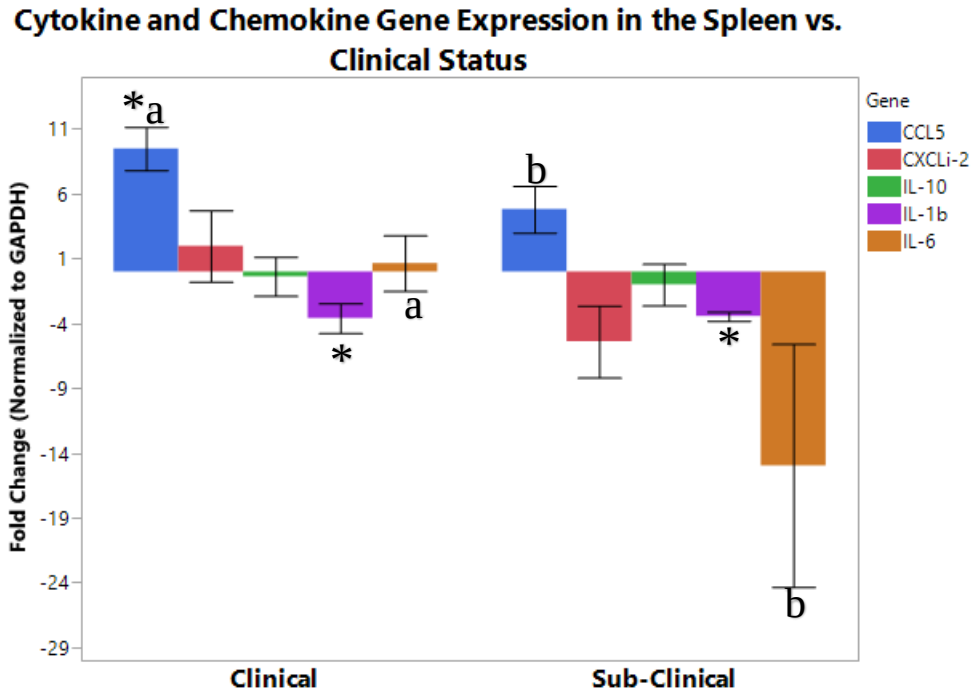

Figure 40. Cytokine and chemokine gene expression in the spleen *vs.* clinical status. "*" denotes significant difference from controls. "a/b" denotes significant difference between clinical and sub-clinical groups. P-values <0.05 were considered to be significant.

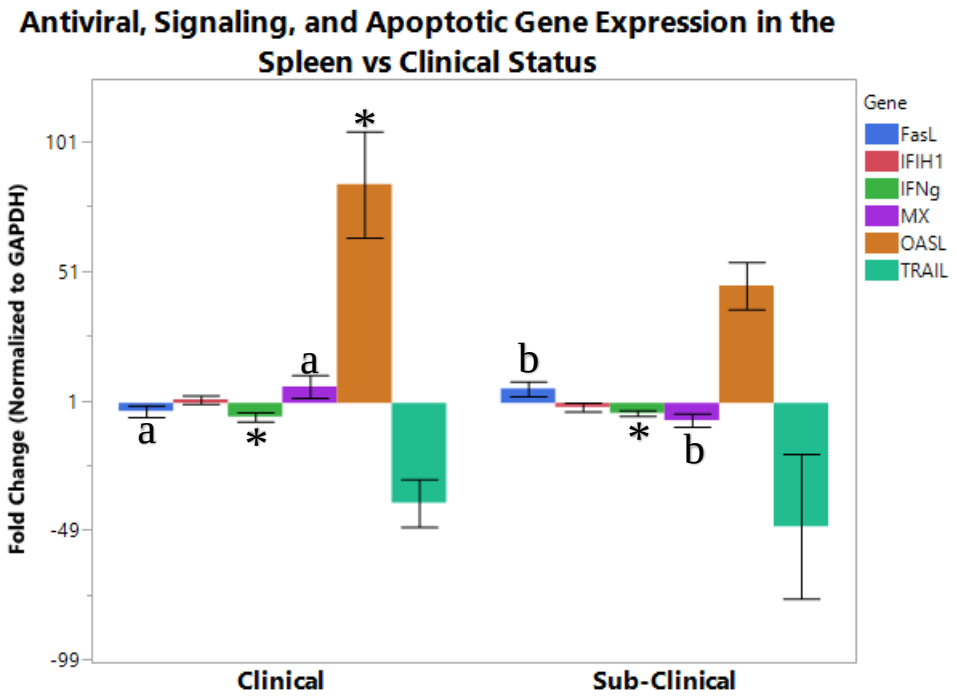

Figure 41. Antiviral, signaling, and apoptotic gene expression in the spleen *vs.* clinical status. "*" denotes significant difference from controls. "a/b" denotes significant difference between clinical and sub-clinical groups. P-values <0.05 were considered to be significant.

Trachea

No IL-10 data were acquired for the trachea. Like the spleen, the trachea was another very active tissue with regards to changes in cytokine gene expression. IL-6 and IL-1β were significantly downregulated in the positive group, -1.78 and -2.22 fold respectively. CCL5 was upregulated 11.18 fold. Both IFIH1 and IFN-γ were significantly downregulated, -1.93 and -4.98 fold while OASL was upregulated 35.47 fold. Both IL-1β and IL-6 were upregulated in both the clinically, -3.2 and -1.7 fold, and sub-clinically, -1.56 and -1.77 fold, affected groups. CCL5 was significantly upregulated

in the clinically affected birds, 15.28 fold, from the controls and considered statistically different than the sub-clinical group at 7.08 fold, which was also different than the controls. There was a lot of antiviral activity in the trachea. Expression of IFIH1 and IFN-γ was decreased in both the clinical, -1.70 and -5.6 fold, and sub-clinical groups, -2.15 and -4.35 fold. Additionally, OASL was upregulated in both of the groups and considered to be different from each other. The clinical group expressed OASL at 47.78 fold while the sub-clinical expressed OASL at 23.15 fold. See figures 22-24.

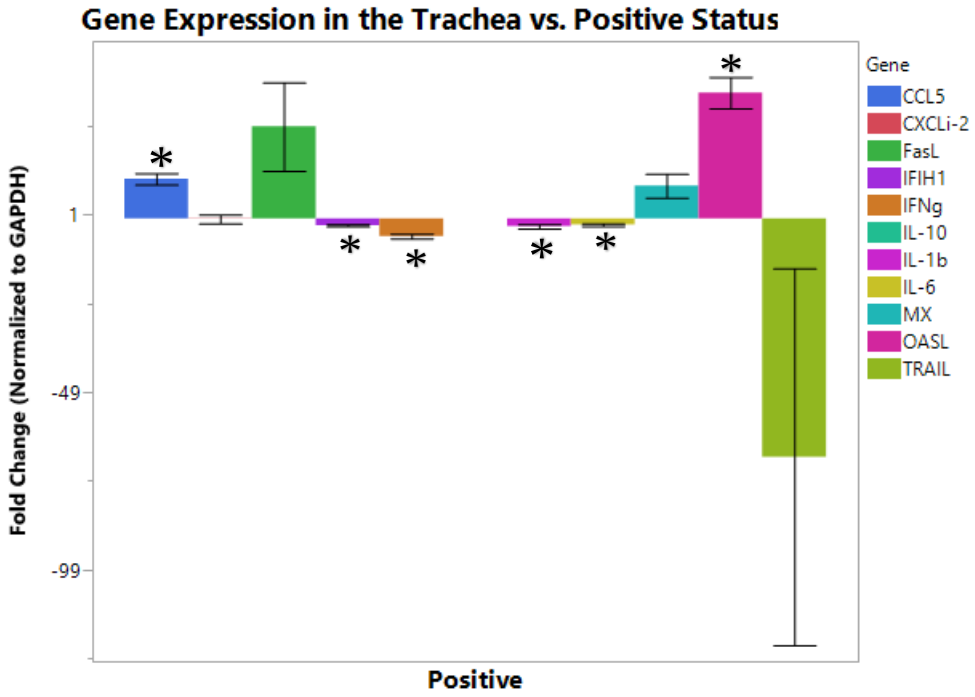

Figure 42. Gene expression in the trachea of positive birds. "*" denotes significant difference from controls. P-values <0.05 were considered to be significant.

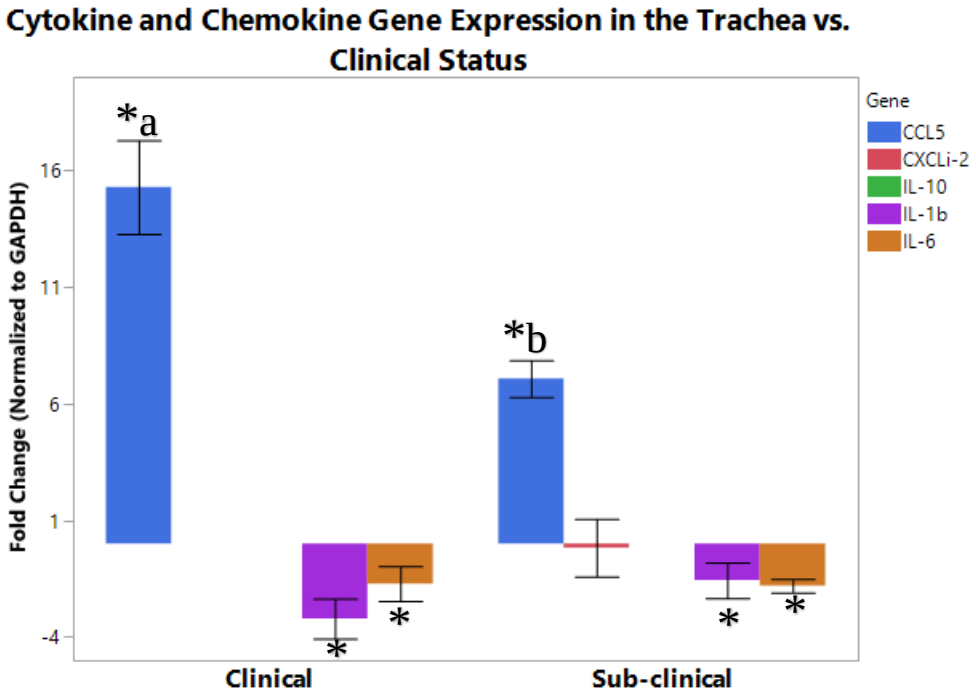

Figure 43. Cytokine and chemokine gene expression in the trachea *vs.* clinical status. "*" denotes significant difference from controls. "a/b" denotes significant difference between clinical and sub-clinical groups. P-values <0.05 were considered to be significant.

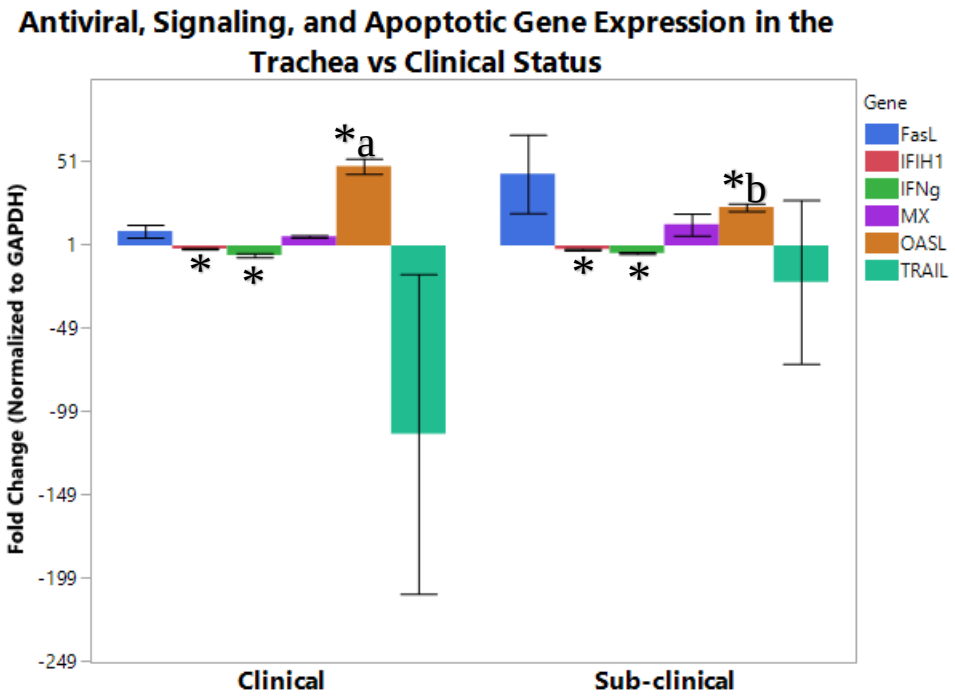

Figure 44. Antiviral, signaling, and apoptotic gene expression in the trachea *vs.* clinical status. "*" denotes significant difference from controls. "a/b" denotes significant difference between clinical and sub-clinical groups. P-values <0.05 were considered to be significant.

Gene Regulation by Positive Status

Pro/Anti-Inflammatory Cytokine and Chemokine Expression

IL-1β was significantly upregulated in the heart but down regulated in the spleen and trachea. IL-6 was upregulated in the brain and heart however downregulated in the trachea. There were no differences detected in IL-10 between the positive birds and negative control birds. CCL-5 was upregulated in the brain, GI, spleen, and trachea. The

spleen and trachea were the most active tissues. CCL-5 was the most active gene in this group of cytokines and chemokines. See Figure 61.

Signaling, Antiviral, and Apoptotic Gene Expression

IFIH1 was upregulated in the heart and liver but downregulated in the trachea of the positive birds. IFN-γ was downregulated in the GI, liver, lung, spleen, and trachea. Mx was only upregulated in the brain while OASL was upregulated in the GI, liver, spleen, and trachea. Expression of neither of the death ligands, TRAIL or FasL, were significantly different in the positive group compared to the negative controls. IFN-γ, and OASL were the most active in this group of signaling, antiviral, and apoptotic genes. (Figure 25).

	Brain	GI	Heart	Liver	Lung	Repro	Spleen	Trachea
Pro-Inflammatory								
IL-1b			*				*	*
IL-6	*		*					*
Anti-Inflammatory								
IL-10								
Chemokine								
CCL5	*	*					*	*
IL-8								
Signal								
IFIH1			*	*				*
Antiviral								
IFNg		*		*	*		*	*
Mx	*							
OASL		*		*			*	*
Apoptotic								
TRAIL								
FasL								

Figure 45. Heat map of gene regulation by positive status. Red indicates significant upregulation and blue indicates significant downregulation. P values <0.05 are considered significant.

Immune Evasion

Based on the cytokine profile of the positive birds, the particular H5N2 virus involved in the outbreak was very efficient at evading the turkey's immune response. It appears that the virus was able to avoid the host's detection immediately upon exposure. The virus was able to avoid detection and suppress any immune reaction in the trachea by downregulating IFIH1 and IFN-γ, thus allowing the virus to move quickly beyond the trachea. Furthermore, IFN-γ was downregulated in the GI, liver, lung, and spleen thus disabling the turkey's ability to fight off the infection. The NS1 protein has been shown to limit the production and effectiveness of the interferons, (Hale et al., 2010), by blocking the cytoplasmic RIG-I/MDA5 signaling cascade or by attenuating INF-inducible signaling (Hale et al., 2010; Vijayakumar et al., 2015). This may be a potential mechanism for downregulating IFN-γ. Although IFN-α and IFN-β were not successfully measured, it is possible that their activity can be *indirectly* measured by the IFN induced antiviral proteins (Ewald et al., 2011), Mx and OASL. Mx was upregulated in the brain and OASL was upregulated in the GI, liver, spleen, and trachea indicating increased IFN activity.

The lack of upregulation of IL-1β, except in the heart where there were pathological lesions, and downregulation in the spleen and trachea indicates an induced lack of inflammatory response. While there was an upregulation of the chemokine/secondary pro-inflammatory mediator, CCL-5, in the brain, GI, spleen, and trachea, it was a secondary response to the presence of the virus in the tissue and

insufficient response. The upregulation of IL-6 in the brain and heart was expected given the neurological and pathological lesions observed at tissue collection. Although the changes in the gene expression of TRAIL, due to high variability, were not statistically significant, the average of TRAIL was always greatly negative, indicating that an induced decrease in apoptosis was possible. The NS 1 protein has been shown to the ability to suppress ligand-mediated apoptosis to increase infectivity in chickens (Xing et al., 2009).

Gene Regulation by Clinical Status

Pro/Anti-Inflammatory Cytokine and Chemokine Expression

IL1-β was upregulated in the lung of the sub-clinical and downregulated in the spleen and trachea of both the clinical and sub-clinical groups. IL-6 was up in the brain of the clinical, heart of both groups, liver of clinical, and down in the spleen of the sub-clinical and trachea of both groups. CCL-5 was up in all tissues of both groups except in the clinical lung, and sub-clinical GI and liver. CXCLi-2 expression was increased only in the lung of the sub-clinical.

Signaling, Antiviral, and Apoptotic Gene Expression

IFIH1 was up in the heart and liver of the clinical and decreased in the trachea of both groups. INF-γ was downregulated in the liver, lung, spleen, and trachea of both groups as well as in the GI of the clinical. Expression was significantly lower in the liver and lung of the clinically affected. A very different phenomenon was seen in the brain,

IFN-γ production was upregulated in the sub-clinical yet downregulated in the clinical. This potentially explains the neurological signs and increased viral load in the clinically affected noted in a previous trial. Mx was upregulated in the GI and spleen of the clinical and downregulated in both tissues in the sub-clinical. OASL expression was significantly upregulated in all tissues except in the sub-clinical brain, GI, and spleen and clinical lung. The upregulation in the heart and trachea was much greater in the clinically affected. OASL is known to aid in the prevention of tissue damage and hyper-inflammatory response and consequently its wide spread upregulation may have contributed to the virus' pathogenesis and immune evasion as indicated by the higher levels in the clinically affected turkeys. There was little significant apoptotic gene expression. FasL was upregulated in the sub-clinical livers and spleen while being down in the clinical spleen. (Figure 26.)

While there were differences noted between the clinical and sub-clinical birds that may explain clinical status and viral load differences, the overall cytokine response difference between the 2 groups is not that remarkable. It is likely that the sub-clinical birds were able to restrict virus replication more effectively than the clinical birds, but all sub-clinical birds were positive and the virus was widespread. Considering the extensive viral presence in all of the tissues, viral loads, and cytokine profile, the sub-clinically affected were most likely only prolonging the inevitable deadly outcome.

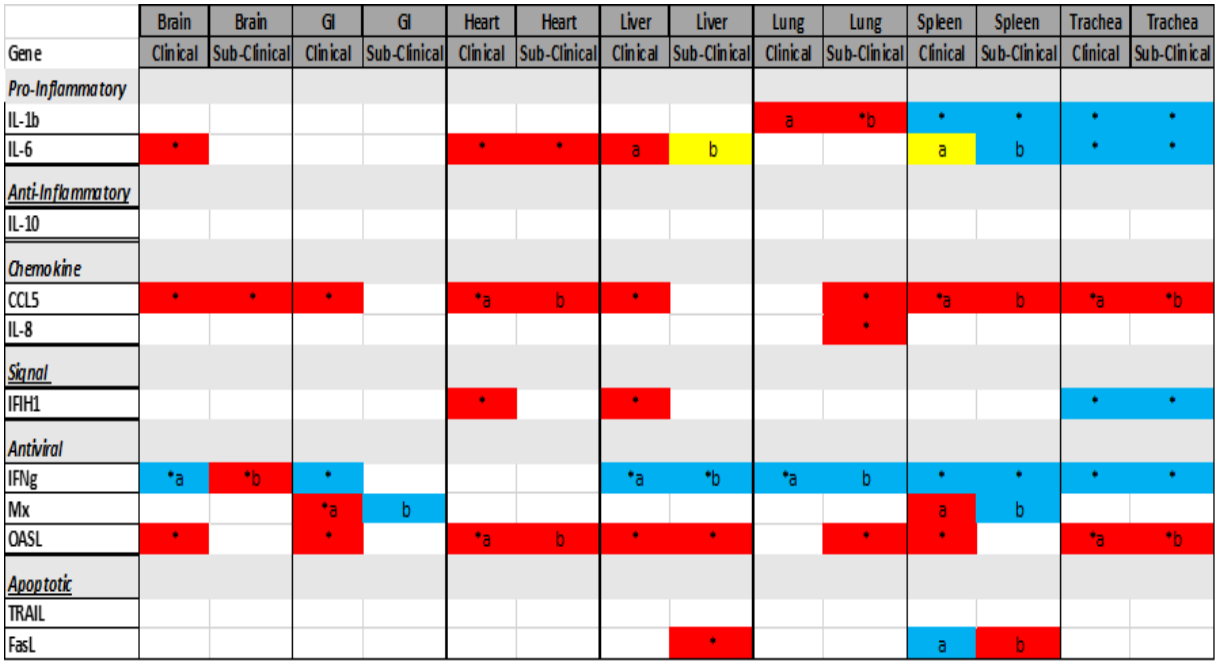

Figure 46. Heat map of gene expression changes by clinical status. Red indicates a significant upregulation, blue a significant downregulation, and yellow indicates no change from the controls. P values <0.05 were considered significant.

Conclusion

While there was some pro-inflammatory response it was not in excess. There is no evidence of a cytokine storm. Death was rather from a lack of a response. This particular virus was very efficient in evading the turkey's immune response. It was able to avoid initial detection by suppressing the expression of viral detecting mechanisms, pro-inflammatory cytokines, and antiviral components in the trachea. Undetected the virus was able to quickly spread throughout the body and replicate very rapidly. The system wide downregulation of IFN-γ and upregulation of CCL-5 and OASL contributed

to the pathogenesis. Death appears to be from organ failure due to viral overload not a cytokine storm.

Both the clinically and sub-clinically affected turkeys had virus in all of the tissues. The clinical differences are most likely the result of viral load in the various tissues, particularly in the brain and spleen. The virus was very efficient at evading detection and, as a consequence, immune defense mechanisms. Some birds were more effective than others in restricting viral replication, hence the differences in viral load of the tissues and subsequent clinical status. Given the system-wide viral distribution and load, the sub-clinical birds were most likely delaying the inevitable fatal outcome.

In general, information regarding HPAIs in experimentally infected turkeys is minimal and information detailing the response of naturally infected turkeys does not exist. Field data from naturally infected turkeys is essential for describing and understanding the disease during an outbreak. Information acquired under experimental conditions cannot be directly equated to what is seen under natural conditions, as route of exposure and environment are not comparable. This study is novel and the first of its kind.

CHAPTER IV

CONCLUSIONS

The outbreak of the highly pathogenic avian influenza virus (HPAI) in 2014-2015 was by far the largest animal disease outbreak in United States history. The turkey industry was the most affected, nearly 70% of the confirmed cases were in turkeys. Despite the massive devastation it caused, very little was known about the specific virus, particularly regarding its distribution and lesions caused within the turkey host during the outbreak. It was unknown as to why there was a very small population of turkeys that would survive the massive mortality and appear unaffected several days later. Some speculated they were perhaps "resistant" to the infection.

All of the birds in the infected barn were infected regardless of clinical status. However, the viral load in the tissues was different in the clinically affected *versus* sub-clinically affected turkeys. The viral load was higher in the brain, GI, spleen, and trachea of the clinically affected birds. The increased viral concentration in the brain most likely contributed to the neurological symptoms observed upon tissue collection. Histological viral lesions were in general very mild and insignificant. The majority of the histological changes were confined to the trachea and liver in the clinically positive birds and primarily consisted of the infiltration of small numbers of heterophils, lymphocytes, and macrophages. This study is the first of its kind that provides virus distribution and semi-quantitative matrix gene analysis across multiple tissues in the turkey. It is also the first

of its kind that characterizes the differences in distribution and matrix gene levels between clinical and sub-clinical birds. The virus appeared to replicate more rapidly in the clinically affected birds, particularly in the brain and reproductive tracts.

There was some pro-inflammatory response noted but it was not in excess. Death does not appear to be the result of a cytokine storm or host response but rather from a lack of response. This particular virus was very efficient in evading the turkey's immune response. It was able to avoid initial detection by suppressing the expression of viral detecting mechanisms, pro-inflammatory cytokines, and antiviral components in the trachea. Undetected the virus was able to quickly spread throughout the body and replicate very rapidly. The system wide downregulation of IFN-γ and upregulation of CCL-5 and OASL contributed to the pathogenesis. Death appears to be purely from viral load in the tissues and subsequent interference with basic physiological functions and not a cytokine storm. While there were differences noted between the clinical and sub-clinical birds that may explain clinical status and viral load differences, the overall cytokine response difference between the 2 groups is not that remarkable. It is very likely that the sub-clinical birds were able to restrict virus replication more effectively than the clinical birds, but all sub-clinical birds were positive and the virus was widespread. Considering the extensive viral presence in all of the tissues, viral loads, and cytokine profile, the sub-clinically affected were most likely only prolonging the inevitable deadly outcome.

Virus was detected in all of the tissues collected on the positive premise, regardless of clinical status thus illustrating its extreme pathogenesis. Generally, histological lesions were minimal and cytokine responses were not in excess. Death does not appear to be the result of organ damage/necrosis or even cytokine storm but purely from immune evasion and excessive viral load in the tissues. Consequently, the high viral loads resulted in organ failure.

Future Research

The results of the trials prompted additional questions that need to be further studied and explained. One of the biggest questions that has yet to be answered is with regards to the exact location of the virus in the tissues. Virus was detected in all of the tissues that were collected yet, minimal pathological and histological lesions were seen. With the help of immunohistochemistry, the exact location of the virus can be located and possibly provide even further insight into the virus and its pathogenesis. In addition, it is unknown as to whether there were any genetic differences between the clinical and sub-clinical birds that may account for the different clinical statuses or susceptibility seen, such as variants of the Mx gene previously described in the chicken (Ewald et al., 2011).

It would be advantageous to further characterize the virulence factors of this particular H5N2 virus and compare it to viruses from other outbreaks. Due to the rapid spread of the disease, it is unlikely that antibodies had time to develop but that avenue

should be explored. Other aspects of the humoral response and characteristics of circulating blood such as viral load have yet to be investigated.

Turkey research is lacking in general due to the cost, time, and equipment required to conduct such research. To my knowledge, there are no published data that describe the changes in gene expression and the dissemination of an HPAI virus in a naturally infected turkey flock. This trial is the first of its kind, therefore there is much more to be explored.

REFERENCES

Abasht, B., Kaiser, M.G., and Lamont, S.J. 2008. Toll-like receptor gene expression in the cecum and spleen of advanced intercross line chicks infected with Salmonella enterica serovar Enteritidis. Vet. Immunol. and Immunop. 123: 314-323.

Abbas, A. K., Lichtman, A.H., and Pillai, S. 2007. Cellular and Molecular Immunology. 6 ed. Saunders Philadelphia

Adams, S. and Sandrock, C. 2010. Avian influenza: update. Med. Princ. Pract. 19: 421-432.

Adams, S.C., Xing, Z., Li, J., and Cardona, C.J. 2009. Immune-related gene expression in response to H11N9 low pathogenic avian influenza virus infection in chicken and Pekin duck peripheral mononuclear cells. Molec. Imm. 46: 1744-1749.

Arsenault, R,J., Trost, B.T., and Kogut, M.H. 2014. A comparison of the chicken and the turkey proteomes and phosphoproteomes in the development of poultry-specific immune-metabolism kinome peptide arrays. Frontiers in Vet. Sc.

Barber, M.R.W., Aldridge, J.R., Webster, R.G., and Magor, K.E. 2010. Association of RIG-I with innate immunity of ducks to influenza. PNAS. 107: 5913-5918.

Barjesteh, N., Behboudi, S., Brisbin, J., Villanueva, A.I., Nagy, E., and Sharif, S. 2014 TLR ligands induce antiviral responses in chicken macrophages. PLOS ONE. 9.

Bertran, K., Swayne, D.E., Pantin-Jackwood, M.J., Kapczynski, D., Spackman, E., and Suarez, D. 2016. Lack of chicken adaptation of novel reassortant North American H5N2 and H5N8 high pathogenicity avian influenza viruses is consistent with restricted poultry outbreaks in Pacific Flyway during 2014-2015. Manuscript submitted for publication.

Blyth, G.A., Chan, W.F, Webster, R.G., and Magor, K.E. 2016. Duck interferon-inducible transmembrane protein 3 mediated restriction of influenza viruses. J. Vir. 90: 103-116.

Brownlie, R. and Allan, B. 2011. Avian Toll-like receptors. Cell Tissue Res. 343: 121-130.

Burggraaf, S., Karpala, A.J., Bingham, J., Lowther, S., Selleck, P., Kimpton, W., and Bean, A.G.D. 2014. H5N1 infection causes rapid mortality and high cytokine levels in chickens compared to ducks. Vir. Res. 185: 23-3.

Cardona, C.J., Xing, Z., Sandrock, C.E. and Davis, C.E. 2008. Avian influenza in birds and mammals. Comp. Immun. Microb. 32: 255-273.

Chen, S., Cheng, A., and Wang, M. 2013. Review- Innate sensing of viruses by pattern recognition receptors in birds. Vet. Res. 44: 82-94.

Davison, F., Kaspers, B., and Schat, K.A. (Editors). 2008. Avian Immunology. Elsevier Ltd. Great Britain.

Eagles, D., Siregar, E.S., Dung, D.H., Weaver, J., Wong, F., and Daniels, P. 2009. H5N1 HPAI in Southeast Asia. Rev. Sci. Tech. Off. Int. Epiz. 28: 341-348.

Ekchariyawat, P., Thitithanyanont, A., Sirisinha, S., and Utaisincharoen. 2011. Apoptosis induced by avian H5N1 virus in human monocyte-derived macrophages involves TRAIL-inducing caspase-10 activation. Innate Imm. 18: 390-397.

Ewald, S.J., Kapczynski, D.R., Livant, E.J., Suarez, D.L., Ralph, J., McLeod, S., and Miller, C. 2011. Association of Mx1 Asn631 variant alleles with reductions in morbidity, early mortality, viral shedding, and cytokine responses in chickens infected with a highly pathogenic avian influenza virus. Immunogen. 63: 363-375

FAO of the United Nations. 2016. AI Situation Update: East and Southeast Asia (October to December 2015)

Gadde, U., Chapman, H.D., Rathinam, T., and Erf, G.F. 2011. Cellular immune responses, chemokine, and cytokine profiles in turkey poults following infection with the intestinal parasite *Eimeria* adenoeides. Poult. Sci. 90: 2243-2250.

Genovese, K.J., He, H., Lowry, V.K., and Kogut, M.H. 2007. Comparison of MAP and tyrosine kinase signaling in heterophils from commercial and wild-type turkeys. Dev. and Comp. Immun. 31: 927-933.

Genovese, K.J., He, H., Lowry, V.K., Swaggerty, C.L., and Kogut, M.H. 2006. Comparison of heterophil function of modern commercial and wild-type Rio Grande turkeys. Avian Pathol. 35: 217-223

Graves, D.T., and Jiang, Y. 1995. Chemokines, a family of chemotactic cytokines. Crit. Rev. Oral Biol Med. 6: 109-118.

Gupta, A.K., Lather, A., and Kumar, T. 2015. Avian cytokines and disease prevention: an overview. J. Cell and Tiss Res. 15: 4761-4764.

Hagag, I.T., Mansour, S.M.G., Zhang, Z., Ali, A.A.H, Ismaiel, E.B.M, Salama, A.A., Cardona, C.J, Collins, J., and Xing, Z. 2015. Pathogenicity of highly pathogenic avian influenza virus H5N1 in naturally infected poultry in Egypt. PLoS ONE 10(5): e0120061.

Hale, B.G., Albrecht, R.A., and Garcia-Sastre, A. 2010. Innate immune evasion strategies of influenza viruses. Future Microbiol. 5: 23-52.

Horimoto, T. and Kawaoka, Y. 2005. Influenza: lessons from the past pandemics, warnings from current incidents. Nature Rev-Microbio. 3: 591-600.

Iwasaki, A. and Pillai, P.S. 2014. Innate immunity to influenza virus infection. Nature Rev- Immuno. 14: 315-328.

Kaiser, P., Rothwell, L., Avery, S., and Balu, S. 2004. Evolution of interleukins. Dev. and Comp. Immun. 28: 375-394.

Kaleta, E.F., and Rulke, C.P.A. 2008. The beginning and spread of fowl plague (H7 high pathogenicity avian influenza) across Europe and Asia (1878-1955). In: Swayne, D.E., editor. Avian Influenza. Ames, IW: Blackwell Publishing. p. 145-190.

Keestra, A.M., de Zoete, M.R., Bouwman, L.I., Vaezirad, M.M., and van Putten, J.P.M.2013. Unique features of chicken Toll-like receptors. Dev. and Comp. Immun. 41: 316-323.

Kapczynski, D.R., Jiang, H., Kogut, M.H. 2014. Characterization of cytokine expression induced by avian influenza virus infection with real-time RT-PCR. In: Spackman, E., editor. Animal Influenza Virus. 2nd edition. New York, NY: Springer. p. 217-233.

Kobayashi, Y., Horimoto, T., Kawaoka, Y., Alexander, D.J., and Irakura, C. 2007. Pathological studies of chickens experimentally infected with two highly pathogenic avian influenza viruses. Avian Pathol. 25: 285-304.

Kogut, M.H. 2000. Cytokines and prevention of infectious diseases in poultry: a review. Avian Pathol. 29: 395-404

Kristiansen, H., Scherer, C.A., McVean, M., Iadonato, S.P., Vends, S., Thavachelvam, K., Steffensen, T.B., Horan, K.A., Kuri, T., Weber, F., Paludan, S.R., and Hartmann, R. 2010. Extracellular 2'-5' oligoadenylate synthetase stimulates RNase L-independent antiviral activity: a novel mechanism of virus-induced innate immunity. J. of Virol. 84: 11898-11904.

Krug, R.M. 2015. Function of the influenza A virus NS1 protein in antiviral defense. Curr Opinion Vir. 12: 1-6.

Kuchipudi, S.V., Tellabati, M., Sebastian, S., Londt, B.Z., Jansen, C., Vervelde, L., Brookes, S.M., Brown, I. H., Dunham, S.P., and Chang, K.C. 2014. Highly pathogenic avian influenza virus infection in chickens but not ducks is associated with elevated host immune and pro-inflammatory responses. Vet. Res. 45: 118-136.

Kuchipudi, S.V., Dunham, S.P., Neli, R., White, G.A. Coward, V.J., Slomka, M.J., Brown, I.H., and Chang, K.C. 2012. Rapid potential of duck cells infected with influenza: a potential mechanism for host resistance to H5N1. Imm. and Cell Bio. 90: 116-123.

Kuribayashi, S., Sakoda, Y., Kawasaki, T., Tanaka, T., Yamamoto, N., Okamatsu, M., Isoda, N., Tsuda, Y., Sunden, Y., Umemura, T., Nakajima, N., Hasegawa, H., and Kida, H. 2013. Excessive cytokine response to rapid proliferation of highly pathogenic avian influenza viruses leads to fatal systemic capillary leakage in chickens. PLOS ONE. 8:7 e68375.

Lee, M.S., Kim, B., Oh, G.T., and Kim, Y.J., 2013. OASL inhibits translation of the type I interferon regulating transcription factor IRF7. Nat. Imm. 14: 346-355.

Li, J., zu Dohna, H., Anchell, N.L., Adams, S.C., Dao, N.T., Xing, Z., and Cardona, C.J. 2010. Adaptation and transmission of a duck-origin avian influenza virus in poultry species. Vir. Res. 147: 40-46.

Liu, C.H., Lin, S.H., Chen, Y.C., Lin, K.C.M., Wu, T.S.J, and King, C.C. 2007. Temperature drops and the onset of severe avian influenza A H5N1 virus outbreaks. PLOS ONE. 2: e191.

Livak, K.J., and Schmittgen, T.D. 2001. Analysis of relative gene expression data using real-time quantitative PCR and the 2-ΔΔCT method. Methods 25: 402-408

Lupiani, B. and Reddy, S.M. 2009. The history of avian influenza. Comp. Immuno Microb. 32: 311-323.

McClain, M.T., Henao, R., Williams, J., Nicholson, B., Tsalik, E.L., Lambkin-Williams, R., Gilbert, A., Mann, A., Ginsburg, G.S., and Woods, C.W. 2015. Differential evolution of peripheral cytokine levels in symptomatic and asymptomatic responses to experimental influenza virus challenge. Clin. Exp. Imm. 183: 441-451.

Mo, I.P., Brugh, M., Fletcher, O.J., Rowland, G.N., and Swayne, D.E. 1997. Comparative pathology of chickens experimentally inoculated with avian influenza viruses of low and high pathogenicity. Avian Dis. 41: 125-136.

Mok, K.P., wong, C.H.K., Cheung, C.Y., Chan, M.C., Lee, S.M.Y., Nicholls, J.M., Guan, Y., and Peiris, J.S.M. 2009. Viral genetic determinants of H5N1 influenza viruses that contribute to cytokine dysregulation. J Infect. Dis. 200: 1104-1112.

Mondal, S., Xing, Z., and Cardona, C. 2013. A comparison of virulence of influenza A virus isolates from mallards in experimentally inoculated turkeys.

OIE- World Organisation for Animal Health. Terrestrial Animal Health Code. Avian influenza. Chapter 10.4.
http://web.oie.int/eng/normes/mcode/en_chapitre_1.10.4.htm

Opal, S.M. and DePalo, V.A. 2000. Anti-inflammatory cytokines. Chest. 117: 1162-1172.

Pantin-Jackwood, M., Wasilenko, J.L., Spackman, E., Suarez, D.L., and Swayne, D.E. 2010. Susceptibility of turkeys to pandemic-H1N1 virus by reproductive tract insemination. Viro. J. 7: 27-29.

Perdue, M.L. 2008. Molecular determinants of pathogenicity for avian influenza viruses. In: Swayne, D.E., editor. Avian Influenza. Ames, IW: Blackwell Publishing. p. 23-41.

Post, J., Burt, D.W., Cornelissen, J. BWJ., Brokes, V., van Zoelen, D., Peeters, B, and Rubel, J. MJ. 2012.. Systemic virus distribution and host responses in brain and intestine of chickens infected with low pathogenic or high pathogenic avian influenza virus. Vir. Journal 9: 61-75.

Powell, F. L., Rothwell, L., Clarkson, M.J., and Kaiser, P. 2009. The turkey, compared to the chicken, fails to mount an effective early immune response to Histomonas meleagridis in the gut. Parasite Immuno. 31: 312-327.

Powell, F. L., Rothwell, L., Clarkson, M.J., and Kaiser, P. 2012. Development of reagents to study the turkey's immune response: cloning and characterization of two turkey cytokines, interleukin (IL)-10 and IL-13. Vet. Immuno. and Immunopath. 147: 97-103.

Rebel, J. MJ., Peeters, B., Fijten, H., Post, J., Cornelissen, J., and Vervelde, L. 2011. Highly pathogenic or low pathogenic avian influenza virus subtype H7N1 infection in chicken lungs: small differences in general acute responses. Vet. Res. 42: 10-21.

Roberts, A.L., Dedadas, S., Zhang, X., Zhang, L., Keegan, A., Greeneltch, K., Solomon, J., Wei, L., Das, J., Sun, E., Liu, C., Yuan, Z., Zhou, J., and Shi, Y. 2003. The role of activation-induced cell death in the differentiation of T-helper subsets. Immunolog. Res. 28: 285-293.

Roth, C.M. 2002. Quantifying gene expression. Current Issues in Mol. Bio. 4: 93-100.

Saif, Y. M. (Editor), 2003. Diseases of poultry. Blackwell Publishing, Ames, IA.

Smith, J., Smith, N., Yu, L., Paton, I.R., Gutowska, M.W., Forrest, H.L., Danner, A.F., Seiler, J.P., Digard, P., Webster, R.G., Burt, D.W. 2015. A comparative analysis of host response to avian influenza infection in ducks and chickens highlights a role for the

interferon-induced transmembrane proteins in viral resistance. BMC Genomics. 16: 574-593.

Sooryanarain, H. and Elankkumaran, S. 2015. Environmental role in influenza virus outbreaks. Annu. Rev. Anim. Biosci. 3: 347-373.

Spackman, E. 2014. Avian influenza virus detection and quantitation by real-time RT-PCR. In: Spackman, E., editor. Animal Influenza Virus. 2nd edition. New York, NY: Springer. p. 105-118.

Stallknecht and Brown. 2008 Ecology of avian influenza in wild birds. In: Swayne, D.E., editor. Avian Influenza. Ames, IW: Blackwell Publishing. p. 43-58.

Suarez, D.L. 2008. Influenza A virus. In: Swayne, D.E., editor. Avian Influenza. Ames, IW: Blackwell Publishing. p. 3-22.

Suarez, D.L. and Schultz-Cherry, S. 2000. Immunology of avian influenza: a review. Dev. and Comp Imm. 24: 269-283.

Suzuki, K., Okada, H., Itoh, T., Tada, T., Mase, M., Nakamura, K., Kubo, M., and Tsukamoto, K. 2009. Association of increased pathogenicity of Asian H5N1 highly pathogenic avian influenza viruses in chickens with highly efficient viral replication accompanied by early destruction of innate immune response. J Vir. 82: 7475-7486.

Swayne, D.E. (Editor), 2008. Avian influenza. Blackwell Publishing, Ames, IA.

Swayne D.E. and Pantin-Jackwood, M. 2008. Pathobiology of avian influenza virus infections in birds and mammals. In: Swayne, D.E., editor. Avian Influenza. Ames, IW: Blackwell Publishing. p. 87-122.

Swayne, D.E. and Suarez, D.L. 2000. Highly pathogenic avian influenza. Office International des Epizooties. 19: 463-482.

Umar, S., Rehman, A., Younus, M.., Qamar-un-Nisa, Ali, A., Shahzed, M., Shah, M.A.A., Munir, M.T., Aslam, H.B., and Yaqoob, M. 2016. Effects of Nigella sativa on immune responses and pathogenesis of avian influenza (H9N2) virus in turkeys. J. App. Poult. Res. 25: 95-103.

Umar, S., Younus, M., Rehmen, M.U., Aslam, A., Shah, M.A.A., Munir, M.T., Hussain, S., Iqbal, F., Fiaz, M., and Ullah, S. 2015. Role of alphatoxin toxicity on transmissibility and pathogenicity of H9N2 avian influenza virus in turkeys. Av. Path. 44: 305-310.

USDA-APHIS. 2015. Avian influenza disease. Modified Nov. 20, 2015. Accessed Jan 2015.
https://www.aphis.usda.gov/wps/portal/aphis/ourfocus/animalhealth/

Vasin, A.V., Temkina, O.A., Egorov, V.V., Klotchenko, S.A., Plotnikova, M.A., and Kiselev, O.I. 2014. Molecular mechanisms enhancing the proteome of influenza A viruses: An overview of recently discovered proteins. Virus Res. 185: 53-63.

Vervelde, L., Reemers, S.S., van Haarlem, D.A., Post, J., Classen, E., Rebel, J. MJ., and Jansen, C.A. 2013. Chicken dendritic cells are susceptible to highly pathogenic avian influenza viruses which induce strong cytokine responses. Dev. and Comp. Imm. 39: 198-206.

Vijayakumar, P., Mishra, A., Ranaware, P.B., Kolte, A.P., Kulkarni, D.D., Burt, D.W., and Raut, A.A. 2015. Analysis of the crow lung transcriptome in response to infection with highly pathogenic H5N1 avian influenza virus. Gene. 559: 77-85.

Wang, J., Tang, C., Wang, Q., Li, R., Chen, Z., Han, X., Wang, J., and Xu, Z. 2015 Apoptosis induction and release of inflammatory cytokines in the oviduct of egg-laying hens experimentally infected with H9N2 avian influenza virus. Vet. Micro. 177: 302-314

Waring P. and Mullbacher, A. 1999. Cell death induced by the Fas/Fas ligand pathway and its role in pathology. Review Article. Imm. and Cell Bio. 77: 312-317.

Wasilenko, J.L., Sarmento, L., and Pantin-Jackwood, M.J. 2009. A single substitution in amino acid 184 of the NP protein alters the replication and pathogenicity of H5N1 avian influenza viruses in chickens. Arch. Virol. 154: 969-979.

Wileman, B. 2015. HPAI in turkey breeder tom semen. Unpub. data. Agforte Willmar, MN.

Xing, Z., Cardona, C.J., Adams, S., Yang, Z., Li, J., Perez, D., and Woolcock, P.R. 2009. Differential regulation of antiviral and proinflammatory cytokines and expression of Fas-mediated apoptosis by NS1 of H9N2 avian influenza virus in chicken macrophages. J. Gen. Vir. 90: 1109-1118.

Xing, Z., Cardona, C.J., Anunciacion, J., Adams, S., and Dao, N. 2010. Roles of the ERK MAPK in the regulation of proinflammatory and apoptotic responses in chicken macrophages infected with H9N2 avian influenza virus. J Gen. Vir. 91: 343-351.

Zhao, G., Gu, X., Lu, X., Pan, J., Duan, Z., Zhao, K., Gu, M., Liu, Q., He, L., Chen, J., Ge, S., Wang, Y., Chen, S., Wang, X., Peng, D., Wan, H., and Liu, X. 2012. Novel reaasortant highly pathogenic H5N2 avian influenza viruses in poultry in China. PLOS ONE. 7: e46183.

Zhang, X.R., Zhang, L.Y., Devadas, S., Li, L., Keegan, A.D., and Shi, Y.F. 2003. Reciprocal expression of TRAIL and CD95L in Th1 and Th2 cells: role of apoptosis in T helper subset. Cell Death and Diff. 10: 203-210.

Zhou, Y.H., Raj, V.R., Siegel, E., and Yu, L. 2010. Standardization of gene expression quantification by absolute real-time qRT-PCR system using a single standard for marker and reference genes. Biomark. Ins. 5: 79-85